Towards understanding the modulation of *in vitro* gastrointestinal lipolysis kinetics through emulsions with mixed interfaces

M.R. INFANTES-GARCIA*, S.H.E. VERKEMPINCK, M.R. SAADI, M.E. HENDRICKX, T. GRAUWET**

Laboratory of Food Technology and Leuven Food Science and Nutrition Research Centre (LFoRCe), Department of Microbial and Molecular Systems (M2S), KU Leuven, Kasteelpark Arenberg 22, PB 2457, 3001 Leuven, Belgium

Author's email addresses:

M.R. INFANTES-GARCIA: marcos.infantes@kuleuven.be

S.H.E. VERKEMPINCK: sarah.verkempinck@kuleuven.be

M.R. SAADI: muhammadreyhan.saadi@student.kuleuven.be

M.E. HENDRICKX: marceg.hendrickx@kuleuven.be

T. GRAUWET: tara.grauwet@kuleuven.be

Journal: Food Hydrocolloids

Submitted: July 2021

21 *author whom correspondence should be addressed during submission process:

22 marcos.infantes@kuleuven.be

23 +32 16 37 65 53

24 ** author whom correspondence should be addressed post-publication:

25 tara.grauwet@kuleuven.be

26 +32 16 32 19 47

Abstract

The functionality of oil-in-water (o/w) emulsions may be modulated by combining emulsifiers rather than using an individual one. Based on our previous studies, citrus pectin (CP) and tween 80 (TW80) were selected as their emulsions presented different physical stability and *in vitro* lipolysis kinetics. Hence, our objective was to design and evaluate the *in vitro* lipolysis kinetics in both the gastric and small intestinal phase of five emulsions containing 5% triolein, 1% CP, and different concentrations of TW80 (0.00625-0.1%). For the initial emulsions, the interfacial load was quantified in terms of CP and TW80 and confirmed that both emulsifiers were present at the interface different ratios as a function of TW80 concentration. These emulsions were subjected to *in vitro* gastric digestion. Oil droplet characterization (particle size and microstructure) revealed a good to excellent physical stability. The kinetics of gastric lipid digestion were modulated by the TW80 concentration in the initial emulsions: higher magnitude of reaction rate constants (rate at which final extent is reached) and extent of lipolysis for lower TW80 concentrations. In addition, the kinetics of gastric lipase adsorption were also correlated with the lipolysis kinetics. In the small intestinal phase, three emulsions were prepared with 1% CP and 0.00625, 0.025 or 0.1% TW80 and *in vitro* digested. All emulsions were completely digested but the rate constant depended on the emulsion gastric stability. Overall, this study proposes an interesting strategy to modulate lipolysis kinetics in the gastric phase, but further research is needed to find another one to modulate small intestinal phase kinetics.

Keywords

Emulsion; *in vitro* digestion; interfacial composition; mixed emulsifiers, gastric lipase; competitive adsorption

1. Introduction

The increasing demand of health-promoting and functional foods influenced the design of food products, including o/w emulsions. O/w emulsions can be employed as a reservoir for essential lyophilic compounds such as polyunsaturated fatty acids, carotenoids and others (McClements, 2018). In addition, emulsions with a long satiety effect could be designed to control food intake (Maljaars et al., 2008). The above nutritional and health-related functions are highly influenced by the kinetics (i.e. rate and extent) of lipid digestion inside the gastrointestinal tract. Lipid digestion is, by nature, an interfacial phenomena. Briefly, lipase adsorption at the oil-water interface is critical for lipid hydrolysis in the gastrointestinal tract (Reis et al., 2009). In this aspect, a possible strategy to modulate the kinetics of lipid digestion is, by manipulating emulsion design properties. For instance, the oil droplet size will govern the available surface area for lipase adsorption and thus the lipid digestion kinetics.

Another important o/w emulsion property that can be tuned to influence lipolysis is the composition of the interface, which refers to the nature of the surface active compounds stabilizing this interface. These surface active compounds can be roughly classified in small surfactants (e.g. tweens, phospholipids or monoglycerides) and biopolymers (e.g. modified starches, proteins or pectin) (Berton-Carabin et al., 2018). During digestion, two important phenomena being influenced by the interfacial composition are *(i)* the droplet physical stability and *(ii)* the competitive adsorption between the initially adsorbed compounds and lipases. The droplet physical stability could be drastically impacted during digestion leading to significant changes in the surface area available for lipase adsorption (Infantes-Garcia et al., 2020; Verkempinck et al., 2018). Next to this, if the surface-active compounds present at the interface form a compact layer, it can block lipase adsorption and hinder/reduce lipid digestion (Muth et al., 2017). This knowledge has been mainly generated from *in vitro* studies due to the advantages they offer (e.g. simplicity and high throughput of samples) (Brodkorb et al., 2019). Nevertheless, most of these studies focused on the evaluation of lipid digestion of emulsions formulated by only a single type of emulsifier.

It can be hypothesized that the functionality, and thus digestion kinetics, of emulsions can be modulated by combining emulsifiers (McClements & Jafari, 2018). In this context, there is limited comprehension of the effect of emulsions having mixed interfaces on the lipid digestion kinetics. Only few studies attempted to explore the lipid digestibility of emulsions prepared with a mix of molecular-based emulsifiers (Dickinson, 2011; Klinkesorn & McClements, 2010; Li & McClements, 2014; Wulff-Pérez et al., 2010). However, these studies did not employ a physiological relevant *in vitro* model (e.g. including a gastric lipolysis step), standardize lipase activities, quantify diverse lipolysis species, nor performed a kinetic analysis of lipolysis based on statistical modeling techniques (especially in the gastric phase).

In two of our previous studies, we evaluated the effect emulsions stabilized by single emulsifiers on the *in vitro* lipolysis kinetics in the gastric and small intestinal phase (Infantes-Garcia et al., 2021a; Infantes-Garcia et al., 2021c). Emulsions stabilized by emulsifiers of different chemical nature showed different physical stability and lipid digestion behaviors under *in vitro* conditions. In the gastric phase, for instance, a citrus pectin (CP) emulsion showed a relatively good stability and the highest extent of lipolysis of all emulsions considered. Another emulsion, which was stabilized by tween 80 (TW80), presented an excellent stability under acidic conditions but gastric lipase was hindered by the compact interfacial layer formed by this small surfactant leading to a negligible extent of lipolysis (Infantes-Garcia et al., 2021a). In the small intestinal phase, the lipolysis kinetics were highly influenced by the emulsions physical stability status at the end of the gastric phase (Infantes-Garcia et al., 2021c).

Based on the previously observed distinct physical stability and lipid digestion behaviors of CP and TW80 during *in vitro* digestion, we hypothesized that these surface-active agents could be combined to generate specific digestion functionalities (e.g. improved gastric physical stability or tailored lipid digestion kinetics). Therefore, our aim was to design and *in vitro* digest five emulsions containing 5% triolein, 1% CP, and five different concentrations of TW80 (0.00625-0.1%). Initial emulsions were characterized in terms of oil droplet properties (i.e. particle size, microstructure and particle charge) and interfacial load of stabilizing agents (CP and TW80). These emulsions were subjected to *in vitro* gastric digestion where

independent samples were taken to evaluate their content of lipolysis products and monitor their oil droplet properties. In addition, the kinetics of gastric lipase adsorption were determined by measuring the interfacial load of this enzyme. In the small intestinal phase, three emulsions were selected (containing 1% CP and 0.00625, 0.025 or 0.1% TW80) and *in vitro* digested using a kinetic approach and their lipid digestion products were determined as well.

2. Materials and methods

2.1 Materials

Triolein (> 99 %) was bought from Acros Organics (Geel, Belgium) and stored at -20 °C with a nitrogen headspace. This very pure oil did not need any further purification since it does not contain any contaminant. This triglyceride can generate regioisomers after hydrolysis. Triolein is found in many commercial oils such as olive, canola and high oleic sunflower oil (Karupaiah & Sundram, 2007). Citrus pectin (CP, degree of methylesterification ≥ 85 %, Sigma-Aldrich, Diegem, Belgium) and tween 80 (TW80, Sigma-Aldrich, Diegem, Belgium) were employed to form mixed interfaces during emulsion preparation. The CP used in this study is a fiber extracted from citrus industry waste streams. Therefore, it can be considered as a sustainable stabilizing agent. In addition, it has shown interesting surface-active properties (Neckebroeck et al., 2020; Verkempinck et al., 2018). Rabbit gastric extract was obtained from Lipolytech (Marseille, France) with measured lipase activity of 12 U/mg (tributyrin as substrate). Pancreatic extract was kindly donated by Nordmark (Uetersen, Germany) and presented a lipase activity of 125 U/mg (tributyrin-based). The remaining HPLC or analytical grade reagents were bought from Sigma-Aldrich (Diegem, Belgium), except for $NaHCO_3$, NaCl, H_2SO_4, KH_2PO_4, ethanol and trimethylamine (Fisher Scientific, Merelbeke, Belgium); KCl, $MgCl_2(H_2O)_6$, acetone, heptane, ethyl acetate and tricholoroacetic acid (Acros Organics, Geel, Belgium); HCl, diethylether and iso-propanol (VWR, Leuven, Belgium); and lipid standards (Larodan, Solna, Sweden).

2.2 Preparation of the emulsions

Our aim was to prepare emulsions containing a mixed interfacial composition with both CP and TW80 adsorbing to the interface. One should consider that biopolymers and small surfactants have different adsorption rates during emulsion formation due to the higher surface activity of the latter ones. Therefore, we decided to perform a sequential emulsion preparation: *(i)* prepare a CP (slower adsorption) emulsion , and then, *(i)* mix the CP emulsion with diluted TW80 solutions, allowing the formation of a mixed interface without completely removing CP from the interface. The coarse CP emulsion was prepared by mixing triolein (10 % w/w), CP (2 % w/w) and Milli-Q water (88 % w/w) in a high-shear mixer (Ultra-Turrax T25, IKA, Staufen, Germany) at 13500 rpm for 5 min. Beforehand, CP was separately dissolved in Milli-Q water and left overnight under constant stirring before mixing with the oil. Next, the coarse CP emulsion was homogenized at 100 MPa (one cycle) in a high-pressure homogenizer (Stansted Fluid Power, Pressure cell homogenizer, U.K.) to form a fine emulsion. After homogenization, the CP emulsion was mixed with one of the five TW80 solutions in a ratio 1:1. These mixtures were left under gentle stirring for 1 h. We finally obtained five emulsions containing 5% of triolein, 1% of CP, and TW80 concentrations of 0.00625, 0.0125, 0.025, 0.05 or 0.1 %. All emulsions presented an initial volume-based average particle size d(4,3) ranging between 1.9 and 2.8 μm, showing no signs of polydispersity.

2.3 Static *in vitro* digestion of the emulsions

Our aim was to investigate the impact of emulsions with mixed interfaces on the kinetics of *in vitro* lipid digestion. For this purpose, we utilized the updated standardized protocol of the international network INFOGEST (Brodkorb *et al*., 2019). The INFOGEST protocol suggests the use of static conditions, which means all physiological parameters (e.g. pH or lipase activity) should be set at the beginning of each digestive phase. In multiple studies, static *in vitro* digestion approaches are proven to be very strong in investigating the effect of food design parameters on digestion phenomena, because they allow very efficient standardization of the digestion conditions. Specifically in our study, we aimed to evaluate the lipid digestion behavior as affected by the interfacial composition. The advantage of static *in vitro* methods

is that all physiological conditions are constant, so the digestion behavior of the diverse emulsified systems could be attributed as a time-dependent phenomena only.

Since the kinetics of lipid digestion were analyzed both in the gastric and small intestinal phase, we carried out independent experiments for both phases. A scaled-down version of the INFOGEST protocol was employed as indicated in our previous articles (Infantes-Garcia et al., 2021a; Infantes-Garcia et al., 2021c). Regarding lipase activities, we set a gastric lipase activity of 60 U/mL (tributyrin-based) in the gastric phase and pancreatic lipase activity of 2000 U/mL (tributyrin-based) in the small intestinal phase. In order to analyze the lipolysis kinetics, samples were taken at eight independent digestion moments in each digestion phase (5; 10; 15; 30; 45; 60; 90; 120 min after enzyme addition).

2.4 Monitoring of oil droplet characteristics during *in vitro* gastric digestion

In a separate *in vitro* digestion experiment, fresh samples of initial emulsions and their respective digested samples (only from gastric phase) at 4 different gastric digestion moments (after 15; 30; 60 and 120 min in the gastric phase) were taken to be characterized in terms of particle charge, microstructure, and particle size. These oil droplet properties are important indicators of the emulsion stability during *in vitro* digestion (Infantes-Garcia et al., 2020).

2.4.1 Particle charge

The particle charge (ζ-potential) of oil droplets was measured by means of a dynamic light scattering electrophoresis equipment (Zetasizer NanoZS, Malvern Instruments, Worcestershire, UK). Samples of initial emulsions or chyme were diluted (1:10) with pure Milli-Q water or adjusted to pH 3, respectively before analysis (Infantes-Garcia et al., 2021a). This emulsion property was determined in duplicate per sample type.

2.4.2 Microstructure

Initial emulsions and their respective digested samples were visualized with an optical microscope (Olympus BX-41) fitted with an Olympus XC-50 digital camera (Olympus, Opticel Co. Ltd., Tokyo, Japan). Samples were observed at 40x magnification.

2.4.3 Particle size

The particle size of samples was determined employing a laser diffraction equipment (Beckman Coulter Inc., LS 13 320, FL, USA). Each sample was added into a stirring tank filled with demineralized water and then pumped into the measurement cell. The measurement was based on the intensity and pattern of scattered light inside the cell, where the laser light had a wavelength main illumination source of 750 nm and wavelengths halogen light for Polarization Intensity Differential Scattering (PIDS) of 450 nm, 600 nm, and 900 nm. The Mie model was used to transform the recorded signals into particle size distributions (triolein refractive index of 1.470), which then reported as the volume-weighted mean diameter d(4,3) (Infantes-Garcia et al., 2021a).

2.5 Analysis of lipid digestion products

Lipolysis products from triolein (TAG) cleavage were analyzed during *in vitro* digestion: *sn*-1,2/2,3-diolein (*sn*-1,2/2,3-DAG); *sn*-1,3-diolein (*sn*-1,3-DAG); *sn*-2-monoolein (*sn*-2-MAG); *sn*-1/3-monoolein (*sn*-1/3-MAG) and oleic acid (FFA). Lipids were extracted and quantified according to our previous work (Infantes-Garcia et al., 2021b).

Lipid extraction: Briefly, an sample of 1 mL was placed in a glass tube and mixed with 0.2 mL sulphuric acid (2.5 M), 2 mL ethanol, and 3 mL diethylether:heptane (1:1). The tube was vortexed for 2 min, followed by an end-over-end rotation at 15 rpm for 30 min. Subsequently, the upper non-polar layer was collected in a 5 mL volumetric flask. A second extraction step was performed by adding 1 mL of diethylether:heptane (1:1) into the previous tube, vortexed for 2 min, and agitated in an end-over-end rotator at 15 rpm for 15 min. The upper layer was collected in the same volumetric flask, which was brought to 5 mL by adding

diethylether:heptane (1:1). The lipids extract was filtered (Chromafil PET filters, 0.20 µL pore size, 25 mm diameter) and then kept at −80 °C until analysis.

HPLC-CAD quantification: The extracted sample was injected into an HPLC system (Agilent Technologies 1200 Series, Diegem, Belgium) fitted with a silica column (Chromolith Performance Si, 100–4.6 mm, Merck, Darmstadt, Germany) preserved with a guard column (Merck, Darmstadt, Germany). An external oven (Chromaster 5310, VWR, Hitachi Ltd., Tokyo, Japan) was used to keep the column temperature at 40 °C. Lipids species were eluted by using a quaternary gradient: isooctane (solvent A), acetone:ethyl acetate (2:1 v/v) containing 0.02% (v/v) of acetic acid (solvent B), isopropanol:water (85:15 v/v) containing 7.5% (v/v) of acetic acid and triethylamine (solvent C), and isopropanol (solvent D). Analytes signals were detected in a CAD (Corona Veo, Thermo Fisher Scientific, Geel, Belgium), operated with a gas pressure of 5.5 bar and evaporator temperature of 35 °C. Lipid standards were employed to construct their corresponding calibration curves to identify and quantify each lipolysis product.

The molar concentration of glycerol and residual triolein ($TAG_{residual}$, only for gastric phase) was calculated per digestion moment as explained by Infantes-Garcia et al. (2020). In a nutshell, a molar balance based on reactions about the sequential hydrolysis of triolein was performed to calculate the residual triolein and glycerol.

2.6 Quantification of the interfacial load

The interfacial load of the initial emulsions and their digested samples during the gastric phase was characterized. The interfacial load of CP and TW80 was quantified in the initial emulsions, while the interfacial load of gastric lipase was determined for chyme samples. To accomplish this latter objective, a separate *in vitro* digestion experiment was performed, and samples were taken after 5, 15, 30, and 60 min of gastric digestion. For the initial emulsions and chyme samples, the creamed oil droplets were separated from the aqueous phase using a centrifugation step. CP, TW80, and gastric lipase present in the aqueous phase were quantified (non-adsorbed fraction). The adsorbed fraction (interfacial load) was calculated by

subtracting the non-adsorbed fraction from the concentration of each compound in a reference solution containing the same amount of the compound but not oil. This procedure to determine the interfacial load using a reference solution has been reported before by Nilsson & Bergenståhl (2007).

2.6.1 Separation of oil droplets from the aqueous phase

Oil droplets were separated from the aqueous phase following the procedure of Yao et al. (2018) with some modifications. An amount of approximately '10 g' of emulsion or chyme sample was centrifuged at 10000 g for 30 min at 4 °C (Sigma 4-16KS centrifuge, Sigma, Osterode am Harz, Germany). Afterwards, a creamed layer containing the oil droplets was observed on top. With the help of a syringe, the lower aqueous phase was carefully collected and stored at -40 °C until analysis.

2.6.2 Quantification of pectin in initial emulsions

Pectin in the aqueous phase of the initial emulsions was quantified based on the hydrolysis method of Ahmed & Labavitch (1978), to form galacturonic acid (GalA). Briefly, the hydrolysis was performed by mixing 0.5 mL of the sample with 8 mL H_2SO_4 and 2 mL of demineralized water. This mixture was stirred in an ice bath for 1 hour. Afterwards, the sample was placed inside a 50 mL volumetric flask and an aliquot of 0.6 mL was transferred into a glass tube cooled in an ice bath and mixed with 3.6 mL of cold 0.0125M sodium tetraborate in H_2SO_4. Afterwards, the mixture was vortexed and heated in an oil bath at 100 °C for 5 min. The mixture was immediately cooled down in an ice bath. Once pectin was hydrolyzed into GalA, the latter was determined using the spectrophotometric procedure of Blumenkrantz & Asboe-Hansen (1973). An aliquot of 60 µL of a 0.15% m-hydroxydiphenyl solution (in 0.5% NaOH) was incorporated in the tube and vortexed for 1 min to obtain a pink solution. The optical density at 520nm was measured after 1 min in a spectrophotometer (Genesys 30 Vis, Thermo Fisher, Waltham, MA, USA). In case of the blank, a 60 µL 0.5% NaOH was used instead. The GalA concentration (mg/mL) was determined using a calibration curve of monogalacturonic acid standard.

2.6.3 Quantification of Tween 80 in initial emulsions

TW80 was also quantified in the aqueous phase of the initial emulsions following the HPLC-Evaporative light scattering detector (ELSD) procedure of Mondal et al. (2020) with some modifications. The surfactant TW80 is composed by a family of compounds. In this aspect, the above mentioned method is capable of eluting all these compounds in a single peak. In our case, we followed the reverse phase HPLC separation procedure by Mondal et al., but the detection was done by a Charged Aerosol Detector (CAD) instead of a ELSD. First, the aqueous phase of the emulsion was filtered (Chromafil PET filters, 0.20 μm pore size, 25 mm diameter), and then injected into the HPLC system (Agilent Technologies 1200 Series, Diegem, Belgium) fitted with a C18 column (Agilent InfinityLab Poroshell 120, 250mm×4.6 mm; 4 μm). The separation was performed using the following mobile phases: acetonitrile, water, and tetrahydrofuran, at 1 mL/min flowrate. We employed exactly the same gradient program as in the original method (Mondal et al., 2020). For the detection and quantification, a CAD was utilized at an evaporator temperature of 50 °C and gas pressure of 5.5 bar. A chemical standard of TW80 does not exist as such due to the diversity of chemical species that are generated during the production of this surfactant. Therefore, the quantification of this compound family in the emulsions was done by constructing a calibration curve using the commercial TW80.

2.6.4 Quantification of gastric lipase during *in vitro* gastric digestion

The adsorbed gastric lipase was quantified as a function of gastric digestion time using a sandwich ELISA kit specific for rabbit gastric lipase (RGL) (MyBiosource, USA). The micro ELISA plate in the kit was pre-coated with an antibody specific to RGL. Either standards or samples were transferred to the micro ELISA plate wells reacting with the specific antibody. Subsequently, a biotinylated detection antibody specific for RGL and Avidin-Horseradish Peroxidase (HRP) conjugate were pipetted into each well and incubated at 37 °C . Then, the substrate solution was pipetted to each well. Only those wells containing RGL, biotinylated detection antibody, and Avidin-HRP conjugate turned blue. Finally, the enzymatic reaction was inhibited by adding a stop solution, which was evidenced by a yellow color. The optical density was

measured at 450 nm. The concentration of RGL in the chyme samples was calculated by comparison with the standard curve.

2.7 Statistical analysis and modeling

2.7.1 One-way ANOVA and comparison test

The volume-weighted mean droplet size and ζ-potential evolution during *in vitro* gastric digestion were statistically compared. Therefore, we performed one-way ANOVA and Tukey HSD comparison analyses to determine significant differences ($P < 0.05$) using the statistical software JMP (JMP pro14, SAS Institute Inc., Cary, NC, USA).

2.7.2 Single-response kinetic modeling

The lipid digestion behavior of the emulsions with mixed interfaces was assessed by single-response modeling using the software JMP (JMP pro14, SAS Institute Inc., Cary, NC, USA). for both the gastric and small intestinal phase, the response was the percentage of TAG digested during *in vitro* digestion. Specifically for the gastric phase, the model that best fitted the data was the modified Gompertz equation (Zwietering et al., 1990). This is a sigmoidal model expressed by equation (1).

$$\%\text{TAG HYD}(t) = \text{TAG HYD}_f \exp\left\{-\exp\left[\frac{k \exp(1)}{H_f}\left(t_{lag} - t\right) + 1\right]\right\} \quad (1)$$

In equation (1), the parameter %TAG(t) is the percentage of digested TAGs at a time t (min); TAG_f (%) is the asymptotic value of digested TAGs ($t = \infty$); k (min^{-1}) is the reaction rate constant; and t_{lag} (min) is the lag time before the cleavage of TAGs starts increasing.

In case of the small intestinal phase, a fractional conversion model was selected to model the data (Salvia-Trujillo *et al*., 2017). The kinetic parameters estimated with this technique are specified in equation (2). In this case, C (%) is the predicted response at time t during the gastric phase; C_f (%) represents the estimated plateau value; and k (min^{-1}) is the estimated reaction rate constant of the evaluated process.

283 $$C = C_f\ (1 - e^{-kt}) \quad (2)$$

284 The estimated kinetic parameters (C_f (%) and k (min^{-1})) were compared by calculating confidence intervals
285 (95 %). This fractional conversion equation was also applied to model the kinetics of gastric lipase
286 adsorption (Section 2.7.4).

287 **2.7.3 Multi-response kinetic modeling**

288 A multi-response kinetic approach was used to obtain advanced insight into the reaction mechanisms of
289 gastric lipolysis. In our recent studies, a reaction scheme was proposed and validated as an *in vitro* gastric
290 lipolysis mechanism (Infantes-Garcia et al., 2020, 2021a). This reaction consists of several enzymatic and
291 interesterification reactions and is shown in Scheme 1. In the present study, the kinetic data sets of the
292 gastric phase study were fitted with this reaction scheme to validate the model.

293 $$\mathrm{TAG} + \mathrm{H_2O} \xrightarrow{k_1} sn\text{-}1,2/2,3\text{-DAG} + \mathrm{FFA}$$

294 $$\mathrm{TAG} + \mathrm{H_2O} \xrightarrow{k_2} sn\text{-}1,3\text{-DAG} + \mathrm{FFA}$$

295 $$\mathrm{TAG} + 2\mathrm{H_2O} \xrightarrow{k_3} sn\text{-}2\text{-MAG} + 2\mathrm{FFA}$$

296 $$sn\text{-}1,2/2,3\text{-DAG} \xrightarrow{k_4} sn\text{-}1,3\text{-DAG}$$

297 $$sn\text{-}1,3\text{-DAG} + \mathrm{H_2O} \xrightarrow{k_5} sn\text{-}1/3\text{-MAG} + \mathrm{FFA}$$

298 $$sn\text{-}2\text{-MAG} \xrightarrow{k_6} sn\text{-}1/3\ \mathrm{MAG}$$

299 $$sn\text{-}1/3\text{-MAG} + \mathrm{H_2O} \xrightarrow{k_7} \mathrm{FFA} + \mathrm{GLY}$$

300 Scheme 1: (Bio)chemical reactions postulated to describe the gastric lipolysis mechanism (Infantes-
301 Garcia et al., 2020).

302 In order to validate the model with the current data sets, the (bio)chemical reactions postulated in Scheme 1
303 were transformed into differential equations. The set of differential equations were solved by means of the
304 'proc model' command of the statistical software SAS (version 9.4, SAS Institute Inc., Cary, NC, USA).

We used a variable order, variable step-size backward difference scheme. Parameters (reaction rate constants *k*) were estimated with the full information maximum likelihood (FIML) and the Gauss-Newton minimization methods. Standard options were used with the 'fit' statement, indicating the 'dynamic' option with a convergence criterion of 0.01, and number of iterations equal to maximally 500 (Infantes-Garcia et al., 2020).

3. Results and discussion

3.1 Characterization of oil droplet properties during *in vitro* gastric digestion

In this study, five emulsions were formulated, containing 5% of triolein, 1% of CP as well as TW80 concentrations of 0.00625, 0.0125, 0.025, 0.05 or 0.1 %. As explained in Section 2.2, a two-phase emulsion preparation procedure was followed to assure the formation of an interfacial layer containing both CP and TW80. This section compiles the oil droplet characterization performed for the initial emulsions and during *in vitro* gastric digestion as well. Some stability indicators, such as droplet size and ζ-potential, were determined since emulsion stability is an important phenomenon influencing the kinetics of lipid digestion (Infantes-Garcia et al., 2020).

3.1.1 Microstructure and oil droplet size

Initial emulsions: The oil droplet size and microstructure are complementary indicators of emulsion stability. In this aspect, initial emulsions with mixed interfaces presented a volume-based average particle size d(4,3) ranging between 1.9 and 2.8 μm. The proximity of these last values is advantageous to further discuss the lipolysis behavior since the main structural difference among emulsions is the interfacial composition. In Figure 1, it can be seen that all initial emulsions were very similar in terms of microstructure as no signs of flocculation nor coalescence were observed. A slight decrease in droplet density was observed for the emulsion stabilized by 1% CP and 0.1% TW80 possibly due to the slightly larger number of sub-micron droplets (Figure 2A). This means all initial emulsions reached a good stability status after

preparation, showing no signs of polydispersity. Therefore, no effect of TW80 concentration on the initial droplet size and microstructure was observed because all emulsions were prepared based on a CP emulsion.

During *in vitro* gastric digestion: The microstructure was little affected by the acidic conditions of the gastric phase (Figure 1). The particle size of the emulsions was acid-stable, except for the emulsion containing 0.0065% TW80 which was the lowest amount of TW80 assessed. This latter emulsion presented an increase of the average particle size from around 2 μm to around 8 μm after 120 min of gastric digestion, mainly due to coalescence (Figure 1 and Figure 2F). The particle size distribution also confirmed the high acid stability of most emulsions (Figures 2A-E). In our previous study, we evaluated the physical stability of emulsions with different interfacial compositions (Infantes-Garcia et al., 2021a). Among them, two emulsions individually stabilized by CP and TW80 were monitored during *in vitro* gastric digestion. The TW80-based emulsion was completely stable, while the CP-based emulsion showed an average particle size increase to ~12 μm during gastric digestion. On the one hand, TW80 is known to be unaffected by the acidic environment in the gastric phase because it is a non-ionic surfactant (Verkempinck et al., 2018). On the other hand, the ionic biopolymer CP is susceptible to changes in pH and ionic strength causing changes in emulsion stability. In the present study, when TW80 at different concentrations was incorporated, the physical stability under gastric conditions was significantly improved compared to an emulsion stabilized by only CP. CP stabilization mechanism is based on electrostatic repulsion (Ngouémazong et al., 2015). Under *in vitro* gastric conditions, CP is susceptible to instability due to the acid pH and ionic strength because the gastric pH is close to CP pKa. Therefore, we anticipate that the incorporation of TW80 to the CP interfacial film progressively shifted the stabilization mechanism towards steric repulsion. In other words, a synergistic effect between CP and TW80 seemed to take place. This was possible because TW80 is a non-ionic surfactant, so it did not electrostatically interact with the ionic CP molecules at the oil-water interface (Guzmán et al., 2016).

3.1.2 Oil droplet electrical charge

The ζ-potential of freshly prepared emulsions and during *in vitro* gastric digestion was evaluated, and is depicted in Figure 2G. The particle charge measurement is an important stability indicator for emulsions stabilized by ionic stabilizing agents, such as CP.

Initial emulsions: All emulsions with mixed interfaces presented negative ζ-potential magnitudes since CP was adsorbed at the oil-water interface. Even though the carboxylic groups in the CP employed in this study were mostly esterified, it still contained a certain number of free carboxylic groups which can be ionized and exhibit a negative charge (Ngouémazong et al., 2015). In addition, there is a clear inverse relation between the concentration of TW80 added to the emulsion and the particle charge. In other words, the higher the TW80 concentration, the less negative the particle charge was. In our previous study (Infantes-Garcia et al., 2021a), we also determined the ζ-potential of emulsions individually stabilized by TW80 and CP. The TW80-based emulsion presented a ζ-potential very close to zero, while the CP-based emulsion presented a value of -20 mV (Infantes-Garcia et al., 2021a). Therefore, these intermediate values of ζ-potential for the emulsions with mixed interfaces may reflect the partial displacement of CP molecules from the oil-water interface, specifically for TW80 concentrations of 0.05 and 0.1%. This probably means that the use of TW80 concentration higher than 0.05% in the emulsion led to a higher amount of CP being removed from the interface. Therefore, the ζ-potential was less negative as a function of increasing TW80 concentration.

During *in vitro* gastric digestion: The ζ-potential of emulsions with mixed interfaces under simulated gastric conditions showed a similar decreasing trend. At low TW80 concentrations (≤0.025 %), the ζ-potential first increased upon addition of positive ions in the simulated gastric fluid, when the pH was reduced. The droplet charge rapidly decreased after 15 min of digestion, then it presented a slight decrease over digestion time. This is due to a fast production of fatty acids after 15 min of digestion followed by a more progressive release of this compound later on. For higher TW80 concentration emulsions (0.05 and 0.1 %), the ζ-potential was closer to zero because a little amount of CP was most likely still adsorbed at the

interface. Then, the droplet charge progressively decreased because the release of fatty acids probably occurred more gradually. Something interesting to notice is the extent to which the particle charge was decreased. This may be an indicator of the lipolysis extent taking place during *in vitro* gastric digestion. For example, the emulsion containing 0.00625% TW80 reached a more negative ζ-potential after 120 min of digestion compared to the emulsions with 0.1% TW80 and could be directly related to the amount of fatty acids formed (39 compared to 12 μmol oleic acid/mL, respectively).

3.2 Interfacial load of initial emulsions and during *in vitro* gastric digestion

The interfacial concentration of emulsifiers in the initial emulsions and adsorbed gastric lipase during *in vitro* gastric digestion was evaluated. To reach these aims, oil droplets in the initial emulsions or chyme samples were first separated from the aqueous phase by means of centrifugation (Yao et al., 2018). Afterwards, an aliquot of the aqueous phase containing the non-adsorbed compounds was taken. CP, TW80 or rabbit gastric lipase were then quantified in the aqueous phase and compared to solutions containing these compounds at the same concentration. By difference, the adsorbed compounds were determined either in the initial emulsions or during *in vitro* gastric digestion.

3.2.1 Adsorbed CP and TW80 in initial emulsions

The interfacial load of the stabilizing agents employed during emulsion preparation was determined to know the final interfacial composition for each of the five CP and TW80 containing emulsions. Figure 3A shows the interfacial load of CP and TW80 (y-axes) in emulsions prepared with 1% CP and different concentrations of TW80 (x-axis). The interfacial load of CP was close to the values determined for other carbohydrates employed as stabilizing agents such as hydrophobized starch (Nilsson & Bergenståhl, 2007), galactoglucomannans, corn fiber gum, and gum Arabic (Mikkonen et al., 2016). The experimental data shown in this Figure 3A confirmed that all five emulsions contained CP and TW80 at the interface, yet at different proportions. As anticipated, it can be observed that as the concentration of TW80 increased during emulsion preparation, the interfacial load of TW80 increased and the one of CP decreased. This is a logic finding since TW80 is considered a higher surface active emulsifier compared to the CP biopolymer

401 (McClements & Jafari, 2018). Therefore, partial displacement of CP from the oil-water was anticipated by
402 TW80 molecules resulting in an interface composed by both compounds.

403 This phenomenon discussed above, is called orogenic displacement and has been observed before in oil-
404 water interfaces composed of milk proteins and tween 20 (Mackie et al., 2000). In the study by Mackie et
405 al., atomic force micrographs and surface tension measurements revealed that the displacement mechanism
406 consisted of three steps. In the first step, small regions of adsorbed surfactant are formed into small defects
407 of the polymer film, without affecting the interfacial layer formed by the polymer. In the second stage, the
408 surfactant domains grow, while it displaces the polymer from the interface. In the third and final step, the
409 polymer layer collapses and is totally removed from the interface if the surfactant concentration is high
410 enough (Mackie et al., 1999). In sum, the disturbance of the polymer film by the surfactant strongly depends
411 on the amount of surfactant present in the system. This mechanism could also explain the trend observed
412 in Figure 3A for the emulsions formed by CP and TW80 since CP is also a surface-active biopolymer. In
413 the present study, a total displacement of CP molecules from the interface did not occur as the TW80
414 concentration added was never high enough to induce this complete removal. It can be hypothesized that
415 only small regions of surfactant were formed for the emulsions containing TW80 concentrations ranging
416 from 0.00625 until 0.025%. This statement is based on the proportions of TW80 and CP for these three
417 emulsions, and the very similar interfacial load of CP found in these emulsions versus the emulsion
418 stabilized by only CP. When the TW80 concentration increased (0.05 and 0.1%), adsorbed TW80 regions
419 grew, initiating the partial removal of CP. Displacement of sugar beet pectin from the air-water interface
420 by Tween 20 was also reported in a previous study (Gromer et al., 2009). This study employed atomic force
421 microscopy to observe the 'holes' located over the pectin interfacial film in which the surfactant was
422 adsorbed. However, only one Tween 20 concentration was utilized to perform this analysis in the cited
423 work.

3.2.2 Adsorbed gastric lipase during *in vitro* gastric digestion

The interfacial load of rabbit gastric lipase (RGL) was determined for the emulsions stabilized by only CP and mixed interfaces, so containing both CP and TW80. To the best of our knowledge, this is the first time this type of experiment was performed at the level of the gastric phase in an *in vitro* study.

In Figure 3B, the evolution of gastric lipase interfacial load over gastric digestion time is depict for the different emulsions. There is a clear effect of the interfacial composition on the kinetics of RGL adsorption. If one compares the adsorption kinetics of the emulsion stabilized by only CP with the ones having a mixed interface, it can be observed that the former one allowed a very fast adsorption of RGL, almost immediately reaching a plateau value after 5 min of gastric digestion. In a previous study, it has been claimed that other biopolymers (e.g. proteins) did not represent a barrier for pancreatic lipase adsorption based on interfacial tension experiments (Maldonado-Valderrama et al., 2013). As mentioned in Section 3.2.1, interfacial films composed of biopolymers contain small defects that can allow adsorption of surface-active compounds with smaller molecular size, such as RGL. Hence, a similar behavior can be expected as compared to the interfacial layer formed by only CP.

The comparison can also be done based on the variable TW80 concentrations. When the TW80 concentration in the emulsion is higher, the adsorption kinetics of RGL slowed down and reached a lower extent of lipase adsorption. Nevertheless, the RGL adsorption kinetics seemed not to be significantly affected when concentrations lower than 0.0125% TW80 or higher than 0.05% TW80 were employed to prepare emulsions. After comparing Figures 3A and 3B, it can be deduced that the main factor modulating RGL adsorption was the interfacial load of TW80 and CP. In this aspect, a low but similar interfacial load was determined in emulsions containing 0.00625 versus 0.0125% TW80, and a higher but rather similar interfacial load was quantified for the emulsions including 0.05 versus 0.1% TW80. This could explain the comparable RGL adsorption behavior in both cases. We found that different TW80 concentrations effected the adsorption kinetics of gastric lipase. An explanation for this phenomena is the competitive adsorption between gastric lipase , CP and TW80. A property that could be used to compare the surface activity of

these compounds is the equilibrium surface pressure (π), which is measured at the water-air interface. The higher magnitude of π, the higher surface-active is the compound. In this case, gastric lipase (π ~ 20 mN/m, Bourlieu et al., (2016)) presents a similar surface activity compared to CP (π= 19-20 mN/m, Baldino et al. (2018)), but lower than TW80 (π=25- 28 mN/m, Rabe et al. (2020)). Since TW80 is a high surface-active molecule with the capacity to hinder gastric lipase adsorption, a higher interfacial load of this surfactant restricts more the access of the enzyme to the interface. Therefore, the competitive adsorption most likely took place between CP and gastric lipase. Similar findings were reported a previous study in which the adsorption of pancreatic lipase was influenced by the concentration of TW80 in emulsions subjected to *in vitro* small intestinal digestion (Yao et al., 2018).

3.3 Kinetic modeling of *in vitro* lipid digestion: Gastric phase

Triolein (TAG) and its hydrolysis products *sn*-1,2/2,3-diolein (*sn*-1,2/2,3-DAG); *sn*-1,3-diolein (*sn*-1,3-DAG); *sn*-2-monoolein (*sn*-2-MAG); *sn*-1/3-monoolein (*sn*-1/3-MAG) and oleic acid (FFA) were quantified during *in vitro* gastric digestion (Figure 4A-G). Our HPLC-CAD technique permitted the separation of regioisomers of MAGs and DAGs (Infantes-Garcia et al., 2021). As a first kinetic approach, we employed single-response modeling to evaluate the lipid digestion behavior of the emulsions stabilized by mixed interfaces (Section 3.3.1). A second kinetic modeling technique used, was the multi-response modeling which allowed to validate the lipolysis mechanism proposed in our previous work (Infantes-Garcia et al., 2020). Additionally, further explanation on the trends observed for the lipolysis products is given in combination with the multi-response modeling description (Section 3.3.2).

3.3.1 Single-response modeling

This empirical modeling approach was utilized to evaluate the effect of the mixed interfacial composition on the gastric lipolysis behavior. The selected response for this modeling process was the % of triolein digested since these molecules are the main substrate for lipases. For this purpose, the model used was the modified Gompertz equation (Eq. 2), in which three parameters were estimated: the lag time (t_{lag}, min), the maximum reaction rate constant (k, min^{-1}), and the asymptotic value of digested TAG (TAG_f, %). This

equation was chosen after a model discrimination process, selecting the simplest model giving the best fit and allowing relevant parameter interpretation. The results of this single response modeling approach, are represented in Figure 4H, while the estimated parameters are presented in Table 1.

Figure 4H shows a lag phase taking place (t_{lag}) during the early phase of the *in vitro* gastric digestion. This lag phase indicates the period before the % of digested TAG begins to rise. It can be observed that the magnitude of t_{lag} is higher for increasing TW80 concentrations in the emulsions. This relation can be quantitatively compared in Table 1, where t_{lag} appears in magnitudes ranging between 5.81 and 16.45 min. The reason behind this behavior can be explained by the interfacial load of CP and TW80. In our previous study, a emulsion stabilized by only CP presented very fast kinetics of TAG cleavage while a TW80-based emulsion showed a very limited digestion (~2 %) during an *in vitro* experiment with the same gastric conditions (Infantes-Garcia et al., 2021a). In this previous research, no lag phase was observed for the kinetic curve of the CP-based emulsion. However, in the present study, the presence of TW80 at the interface modulated the adsorption of gastric lipase (Section 3.2.2). Therefore, limited TAG hydrolysis occurred during the first minutes of *in vitro* gastric digestion, especially for the emulsions prepared with higher TW80 concentrations (> 0.025% TW80). For these latter emulsions, a stronger competitive adsorption effect between gastric lipase, CP, and TW80 probably took place leading to a lower initial enzyme adsorption. The surfactant TW80 exhibits a higher surface activity compared to gastric lipase, thus modulating its adsorption.

The reaction rate constant (k, min^{-1}) of TAG digestion indicates the rate with which the final extent of digestion was reached. This parameter was also influenced by the TW80 concentration present at the oil-water interface. As observed in Table 1, the magnitudes of k varied between 0.32 and 1.64 min^{-1} for the different emulsions. There is a clear inverse relation between this kinetic parameter and the TW80 concentration in the emulsions. In other words, the emulsion containing the lowest TW80 concentration showed the highest rate of TAG cleavage and vice versa. In this case, the kinetics of gastric lipase adsorption also played a critical role since the interfacial load of this enzyme determined the rate with which the

substrate TAG was hydrolyzed. In emulsions with higher concentrations of TW80, there was a higher competitive adsorption effect as compared to emulsions with lower load of TW80 at the interface. The amount of TW80 present at the interface determined the interfacial load of gastric lipase which modulated the lipid digestion reaction rate constant during the gastric phase (cfr. Section 3.2.2)..

The extent of gastric lipolysis (TAG HYD_f) was evidently modulated by the load of TW80 at the interface. This kinetic parameter is an indication for the termination of the lipid digestion process. In the gastric phase, the leveling off of TAG HYD_f happened due to the entrapment of gastric lipase at the interface. This phenomenon has been reported before and occurs because lipolysis products, mainly fatty acids, accumulate at the interface and entrap gastric lipase (Pafumi et al., 2002). The absence of bile salts in the gastric phase provokes this fatty acids accumulation at the interface. The different extents of TAG cleavage shown in Table 1 are directly linked to the kinetics of gastric lipase adsorption, specifically to the final interfacial load of this enzyme (Section 3.2.2). If Figures 3B and 4H are compared, the kinetics of lipase adsorption and digested TAG are very similar. The explanation for this similarity is related to the extent of gastric lipase adsorption. For instance, when this extent was lower, it led to a faster entrapment of this enzyme because a lower interfacial concentration of fatty acids was needed to entrap it (Pafumi et al., 2002). Thus, a faster entrapment of gastric lipase caused a lower final extent of TAG digestion in the gastric phase.

The single-response approach used in this section permitted the comparison of the lipolysis behaviors of emulsions stabilized by mixed interfaces. However, the trends followed by the lipolysis products shown in Figure 4A-G are an indication that more complex interrelated reactions are taking place. Then, a more powerful statistical technique, multi-response modeling, was utilized in the next section to validate the gastric lipolysis mechanism that our research group proposed before.

3.3.2 Multi-response modeling

Multiple lipid digestion species were quantified as shown in Figure 4A-G. These lipolysis products included a substrate (TAG), intermediate products (DAGs and MAGs), and final products (FFA and GLY). These compounds can be treated as responses which are part of a common network of (bio)chemical reactions. In

order to elucidate the mechanism behind these reactions, a more advance modeling technique is needed. In one of our recent studies, multi-response modeling was employed to describe the lipid hydrolysis mechanism during *in vitro* gastric digestion (Scheme 1, Infantes-Garcia et al. (2020)). This proposed model was further validated with independent data sets in another recent study form our research group (Infantes-Garcia et al., 2021a). In our two previous studies, the model was applied in emulsions stabilized by a single emulsifier and were *in vitro* digested under the same gastric conditions. In the present research, we aimed to prove whether the multi-response model can be also applied when emulsions stabilized by mixed interfaces are subjected to *in vitro* gastric digestion.

The first step followed during the modeling process was to translate the chemical reactions from Scheme 1 into differential equations. These equations included the reaction rate constants ($k_{1\text{-}7}$) and the extent of TAG cleavage (TAG_f) (Figure A, Supplementary material). Afterwards, the kinetic parameters were estimated by solving the differential equations using the software SAS. The model output was evaluated following these criteria: convergence of the model, the adjusted determination coefficient (R^2_{adj}), the standardized residual plots, and the parameter estimates error. The five data sets obtained in this study were subjected to the modeling process, resulting in the convergence of the model for all of them. The R^2_{adj} and residual plots showed a good to excellent goodness of fit (Table A and Figure B in Supplementary material, respectively). Something important to highlight is that the whole set of experimental data (i.e. starting from 0 min) was not included in the analysis due to the presence of a lag phase. This lag phase caused either lack of convergence or bad fit for some responses. Therefore, it was decided that the data sets corresponding to emulsions containing 0.00625 and 0.0125% TW80 included experimental points only from 5 min of gastric digestion, while the analysis of other three data sets started after 10 min.

Figure 5 shows the representation of the multi-response modeling performed for the five data sets generated in this work. It can be observed that the hydrolysis of TAG molecules first led to the formation of intermediate products (i.e. DAG and MAGs). Since gastric lipase is stereospecific for the *sn*-3 position, the main intermediate product was *sn*-1,2/2,3-diolein (racemic mixture). We anticipate that this racemic

549 mixture majorly contains the stereoisomer *sn*-1,2-diolein as reported before in an *in vitro* study involving
550 rabbit gastric lipase (Rodriguez et al., 2008). From Scheme 1, the reactions describing the formation of
551 intermediate products are the ones linked to $k_{1\text{-}3}$. More specifically, the kinetic parameters k_1 and k_3 are
552 biochemical reactions related to the hydrolysis of the *sn*-1/3 positions, while k_2 is related to the cleavage of
553 the *sn*-2 position. Therefore, gastric lipase activity over the *sn*-2 position was detected through the multi-
554 response approach used in this study. This finding has also been reported before by Carrière *et al*. (1997).
555 If one compares k_1 and k_2, the magnitude of the *sn*-1/3 position cleavage is higher compared to the one of
556 the *sn*-2 position. This is a logic finding based on the regioselectivity of gastric lipase (Table 2) (Rogalska
557 et al., 1990). However, the magnitude of k_3 is much lower in comparison to the first two rate constants
558 because TAG hydrolysis is a two-step reaction indicating the preference of gastric lipase for hydrolyzing
559 the extreme positions. An interesting result to highlight is the effect of the TW80 concentration used on the
560 rate constant magnitudes, especially k_1. As explained in Section 3.3.1, the interfacial load of TW80 in the
561 different emulsions modulated the adsorption of gastric lipase, and therefore, the kinetics of gastric lipid
562 digestion including the reaction rate constants. This effect can also be observed in Figure 5, where the trends
563 of TAG hydrolysis and intermediate product formation (until ~60 min of digestion) is clearly influenced by
564 the binary interfacial composition.

565 In most cases, the hydrolysis of TAG stopped after 60 min of gastric digestion which also halted the
566 production of intermediate products. At this point, gastric lipase was probably (almost) completely
567 entrapped by the lipolysis products formed during the first hour of gastric digestion. After this point,
568 intermediate products started to be cleaved to further form the final products, FFA and GLY. The
569 explanation for this phenomenon can be that the lipolysis products surrounding gastric lipase restrict the
570 access to the lipid core containing TAGs (Pafumi et al., 2002). However, these products are still accessible
571 to the enzyme so the hydrolysis is slowed down but still occurred. From Scheme 1, it can be observed that
572 the reactions related to k_5 and k_7 describe the degradation of intermediate products. Similarly as for the
573 hydrolysis of TAGs, the interfacial load of TW80 is influencing the magnitude of the rate constants related

to the intermediate products cleavage, especially on k_5 (Table 2). The reactions related to k_4 and k_6 refer to interesterification reactions which have been reported before (Serdarevich, 1967). Fatty acids located at the *sn*-2 position tend to migrate to the outer ones due to the chemically instability of this central position. These latter reactions are the slowest ones compared to the enzymatic conversions but still contribute to the formation of final products. From Table 2, we found that the magnitude of the rate constants related to the isomerization reactions are not significantly different among each other. This is coherent since emulsion properties should not affect the rate of this type of reactions. The last kinetic parameter in Table 2 is the TAG concentration present at the end of gastric digestion (TAG_f). Similarly as observed in Section 3.3.1, this parameter was significantly influenced by the TW80 concentration present in the initial emulsions.

In sum, a mechanistic insight into the lipolysis reactions was obtained under *in vitro* gastric conditions. We proved that the mechanistic model was valid for data sets generated with emulsions having different design properties. It was also evidenced that the kinetic parameters were modulated by interfaces composed of CP and TW80 at different ratios.

3.4 Kinetic modeling of *in vitro* lipid digestion: Small intestinal phase

Following the kinetic analysis of the gastric phase, a kinetic approach was also applied in the small intestinal phase. In this case, we selected three data sets corresponding to the digestion of emulsions showing the most distinct lipid digestion behaviors in the gastric phase: emulsions stabilized by 1% CP and 0.00625, 0.025 or 0.1% TW80. For these three data sets, only an emperical model was applied and is discussed in this section. We intended to apply the mechanistic approach as well, but unfortunately the data sets did not converge for any reaction scheme tested (data not shown). The reason for this lack of convergence was the very fast kinetics occurring in the first minutes of small intestinal digestion which did not allow a good parameter estimation.

Figure 6A-G shows the evolution of the diverse lipolysis products quantified during the *in vitro* small intestinal digestion of emulsions containing both CP and TW80 at different ratios. As expected, the main

intermediate product of lipid digestion from TAG hydrolysis was *sn*-2-monoolein. The stereoselectivity of pancreatic lipase over the outer positions of the glycerol moiety generated this compound. Even though pancreatic lipase was the main lipase in this digestion phase, gastric lipase was also still active. It has been claimed that this latter enzyme contributes to around 7.5% of digestion in the small intestinal phase (Carrière et al., 1993). This could be the reason why a significant concentration of glycerol was produced by the *sn*-2 activity of gastric lipase. After comparing the formation/degradation of these compounds, it can be claimed that these followed different trends during the first 45 min of small intestinal digestion. This discrepancy can be attributed to the distinct final extents of gastric lipid digestion and probably the slightly different particles sizes reached by the emulsions at the end of the previous gastric phase. The latter hypothesis is further discussed in the following paragraphs where single-response modeling is applied. After 45 min of digestion, the trends followed by the lipolysis products were quite similar because at this point the digestion reached its final stage. In our previous study, lipid digestion product formation of emulsions stabilized by single emulsifiers showed a comparable behavior as in the present study (Infantes-Garcia et al., 2021a). In other words, the lipolysis species followed different behaviors during the first half of the *in vitro* digestion, while later their concentrations were closer to each other.

As previously mentioned, single-response modeling was utilized to quantitatively analyze the kinetics of *in vitro* small intestinal digestion of the three emulsions at issue. The selected response was again the % of TAGs digested, but a three-parameter fractional conversion model was employed this time because it presented the best fit after model discrimination. Figure 7A shows the representation of this kinetic modeling, while Table 3 contains the estimated parameters. The estimated initial concentrations of TAGs (C_0) confirmed that the gastric pre-lipolysis was significantly different for the three emulsions. About the reaction rate constants *k*, one would expect that the emulsion containing 0.00625% TW80 was the fastest in reaching the final extent of digestion because more than 60% of TAGs were already cleaved during the gastric phase. However, this latter emulsion presented the lowest magnitude of *k*, while the other emulsions presented higher magnitudes for the *k* value. An explanation for this phenomenon could be partially related

to the particle size of the emulsions at the beginning of the small intestinal phase. Figure 7B illustrates the correlation between this emulsion property and the rate constants for the three emulsions. There is a clear inverse relation between them indicating that the particle size had a significant influence on the kinetics of TAGs digestion during the first term of *in vitro* small intestinal digestion. Of course, the attribution of the lipolysis behavior to a single emulsion property is an oversimplification of the phenomenon, but this correlation is a first step towards a better understanding of this enzymatic reaction. Table 3 also shows the extent of digestion C_f which resulted in similar values for the three emulsions. We hypothesize that bile salts easily removed the surface-active compounds present at the interface leading to a fast lipolysis kinetics (TAGs digested in less than 30 min) and complete lipid digestion. This efficient displacement of molecular-based interfacial layers by bile salts is probably a mammal evolutionary feature developed to fully digest lipids (Bai et al., 2019). Therefore, the use of emulsions stabilized by mixed interfaces seemed not to have a significant modulation of the small intestine lipid digestion kinetics.

4. Conclusions

This study evaluated the kinetics of *in vitro* lipid digestion in both the gastric and small intestinal phase as impacted by emulsion mixed interfaces. Five emulsions prepared with CP and TW80 were subjected to *in vitro* digestion. We proved that both stabilizing agents were initially present at the interface as determined by the measurement of the interfacial load. The ratio of CP and TW80 at the interface depended on the TW80 amount added during emulsion preparation, resulting into a certain degree of CP displacement from the interface by the surfactant. In the gastric phase, all emulsions presented good physical stability so the lipid digestion behavior could be mainly attributed to the interfacial composition. The kinetic analysis showed that the reaction rate constant and extent of *in vitro* gastric digestion was modulated as a function of the TW80 concentration used to prepare the emulsion. This phenomenon was attributed to the experimentally determined kinetics of gastric lipase adsorption which probably exhibited a stronger competitive adsorption for increasing TW80 concentrations. A mechanistic insight was also obtained through the validation of a multi-response model previously proposed by our research group. The kinetic

parameters of this mechanistic model confirmed previous findings. In the gastric compartment, The contribution of gastric lipolysis on the overall lipid digestion is of major importance for specific population groups (e.g. infants or patients with pancreatic disorders) or to trigger some physiological responses (e.g. satiety signals). In the small intestinal phase, however, lipid digestion kinetics were not influenced by the ratio of CP and TW80 at the interface. Very fast kinetics of lipolysis were observed meaning that single layers composed of CP and TW80 did not hinder the activity of the lipolytic system in the small intestine. These kinetics were partially influenced by the stability status of the oil droplets, more specifically by the oil droplet size at the beginning of the small intestinal phase. Therefore, emulsions with mixed molecular-based emulsifiers were not able to modulate *in vitro* small intestinal lipolysis kinetics. Further research is needed to better understand the modulation of lipid digestion in this digestive phase from an interfacial design perspective. In this aspect, more complex interfaces are probably required to regulate the adsorption of bile salts and pancreatic lipases (e.g. multilayers, particle-based or conjugated interfaces).

Acknowledgement

M.R. Infantes-Garcia is a Doctoral Researcher funded by the Research Foundation Flanders (FWO - Grant No. 1S03318N). S.H.E. Verkempinck is a Postdoctoral Researcher funded by the Research Foundation Flanders (FWO - Grant no. 1222420N). The authors also acknowledge the financial support of the Internal Funds KU Leuven.

Declaration of interests

The authors of this work declare no conflict of interests.

References

Ahmed, A. E. R., & Labavitch, J. M. (1978). A simplified method for accurate determination of cell wall uronide content. *Journal of Food Biochemistry*, *1*(4), 361–365. https://doi.org/10.1111/j.1745-4514.1978.tb00193.x

671 Bai, L., Lv, S., Xiang, W., Huan, S., McClements, D. J., & Rojas, O. J. (2019). Oil-in-water Pickering
672 emulsions via microfluidization with cellulose nanocrystals: 2. In vitro lipid digestion. *Food*
673 *Hydrocolloids*, *96*, 709–716. https://doi.org/10.1016/j.foodhyd.2019.04.039

674 Baldino, N., Mileti, O., Lupi, F. R., & Gabriele, D. (2018). Rheological surface properties of commercial
675 citrus pectins at different pH and concentration. *LWT*, *93*, 124–130.
676 https://doi.org/10.1016/J.LWT.2018.03.037

677 Berton-Carabin, C. C., Sagis, L., & Schroën, K. (2018). Formation, Structure, and Functionality of
678 Interfacial Layers in Food Emulsions. *Annual Review of Food Science and Technology*, *9*(1), 551–
679 587. https://doi.org/10.1146/annurev-food-030117-012405

680 Blumenkrantz, N., & Asboe-Hansen, G. (1973). New method for quantitative determination of uronic
681 acids. *Analytical Biochemistry*, *54*(2), 484–489. https://doi.org/10.1016/0003-2697(73)90377-1

682 Bourlieu, C., Paboeuf, G., Chever, S., Pezennec, S., Cavalier, J.-F. O., Guyomarc 'h, F., Deglaire, A.,
683 Bouhallab, S., Dupont, D., Carrière, F., & Vié, V. (2016). Adsorption of gastric lipase onto
684 multicomponent model lipid monolayers with phase separation. *Colloids and Surfaces B:*
685 *Biointerfaces*, *143*, 97–106. https://doi.org/10.1016/j.colsurfb.2016.03.032

686 Brodkorb, A., Egger, L., Alminger, M., Alvito, P., Assunção, R., Ballance, S., Bohn, T., Bourlieu-
687 Lacanal, C., Boutrou, R., Carrière, F., Clemente, A., Corredig, M., Dupont, D., Dufour, C.,
688 Edwards, C., Golding, M., Karakaya, S., Kirkhus, B., Le Feunteun, S., … Recio, I. (2019).
689 INFOGEST static in vitro simulation of gastrointestinal food digestion. *Nature Protocols*, *14*(4),
690 991–1014. https://doi.org/10.1038/s41596-018-0119-1

691 Carrière, F., Barrowman, J., Verger, R., & Laugier, R. (1993). Secretion and contribution to lipolysis of
692 gastric and pancreatic lipases during a test meal in humans. *Gastroenterology*, *105*(3), 876–888.
693 https://doi.org/https://doi.org/10.1016/0016-5085(93)90908-U

694 Carrière, F., Rogalska, E., Cudrey, C., Ferrato, F., Laugier, R., & Verger, R. (1997). In vivo and in vitro
695 studies on the stereoselective hydrolysis of tri- and diglycerides by gastric and pancreatic lipases.
696 *Bioorganic & Medicinal Chemistry*, *5*(2), 429–435. https://doi.org/10.1016/S0968-0896(96)00251-9

697 Dickinson, E. (2011). Mixed biopolymers at interfaces: Competitive adsorption and multilayer structures.
698 *Food Hydrocolloids*, *25*(8), 1966–1983. https://doi.org/10.1016/j.foodhyd.2010.12.001

699 Gromer, A., Kirby, A. R., Gunning, A. P., & Morris, V. J. (2009). Interfacial Structure of Sugar Beet
700 Pectin Studied by Atomic Force Microscopy. *Langmuir*, *25*(14), 8012–8018.
701 https://doi.org/10.1021/LA900483Z

702 Guzmán, E., Llamas, S., Maestro, A., Fernández-Peña, L., Akanno, A., Miller, R., Ortega, F., & Rubio, R.
703 G. (2016). Polymer-surfactant systems in bulk and at fluid interfaces. In *Advances in Colloid and*
704 *Interface Science* (Vol. 233, pp. 38–64). Elsevier. https://doi.org/10.1016/j.cis.2015.11.001

705 Infantes-Garcia, M. R., Verkempinck, S. H. E., Gonzalez-Fuentes, P. G., Hendrickx, M. E., & Grauwet,
706 T. (2021). Lipolysis products formation during in vitro gastric digestion is affected by the emulsion
707 interfacial composition. *Food Hydrocolloids*, *110*, 106163.
708 https://doi.org/10.1016/j.foodhyd.2020.106163

709 Infantes-Garcia, M. R., Verkempinck, S. H. E., Guevara-Zambrano, J. M., Andreoletti, C., Hendrickx, M.
710 E., & Grauwet, T. (2020). Enzymatic and chemical conversions taking place during in vitro gastric
711 lipid digestion: The effect of emulsion droplet size behavior. *Food Chemistry*, *326*, 126895.
712 https://doi.org/10.1016/j.foodchem.2020.126895

713 Infantes-Garcia, M.R., Verkempinck, S. H. E., Guevara-Zambrano, J. M., Hendrickx, M. E., & Grauwet,
714 T. (2021). Development and validation of a rapid method to quantify neutral lipids by NP-HPLC-
715 charged aerosol detector. *Journal of Food Composition and Analysis*, *102*, 104022.
716 https://doi.org/10.1016/j.jfca.2021.104022

Infantes-Garcia, Marcos R., Verkempinck, S. H. E., Hendrickx, M. E., & Grauwet, T. (2021). Kinetic Modeling of *In Vitro* Small Intestinal Lipid Digestion as Affected by the Emulsion Interfacial Composition and Gastric Prelipolysis. *Journal of Agricultural and Food Chemistry*, *69*(16), 4708–4719. https://doi.org/10.1021/acs.jafc.1c00432

Karupaiah, T., & Sundram, K. (2007). Effects of stereospecific positioning of fatty acids in triacylglycerol structures in native and randomized fats: a review of their nutritional implications. *Nutrition & Metabolism*, *4*, 16. https://doi.org/10.1186/1743-7075-4-16

Klinkesorn, U., & McClements, D. J. (2010). Impact of lipase, bile salts, and polysaccharides on properties and digestibility of tuna oil multilayer emulsions stabilized by lecithin-chitosan. *Food Biophysics*, *5*(2), 73–81. https://doi.org/10.1007/s11483-010-9147-2

Li, Y., & McClements, D. J. (2014). Modulating lipid droplet intestinal lipolysis by electrostatic complexation with anionic polysaccharides: Influence of cosurfactants. *Food Hydrocolloids*, *35*, 367–374. https://doi.org/10.1016/j.foodhyd.2013.06.011

Mackie, A. R., Gunning, A. P., Wilde, P. J., & Morris, V. J. (1999). Orogenic displacement of protein from the air/water interface by competitive adsorption. *Journal of Colloid and Interface Science*, *210*(1), 157–166. https://doi.org/10.1006/jcis.1998.5941

Mackie, A. R., Gunning, A. P., Wilde, P. J., & Morris, V. J. (2000). Orogenic displacement of protein from the oil/water interface. *Langmuir*, *16*(5), 2242–2247. https://doi.org/10.1021/la990711e

Maldonado-Valderrama, J., Terriza, J. A. H., Torcello-Gómez, A., & Cabrerizo-Vílchez, M. A. (2013). In vitro digestion of interfacial protein structures. *Soft Matter*, *9*(4), 1043–1053. https://doi.org/10.1039/c2sm26843d

Maljaars, P., Peters, H., Mela, D., & Masclee, A. (2008). Ileal brake: A sensible food target for appetite control. A review. *Physiology & Behavior*, *95*, 271–281.

https://doi.org/10.1016/j.physbeh.2008.07.018

McClements, D. J. (2018). Enhanced delivery of lipophilic bioactives using emulsions: a review of major factors affecting vitamin, nutraceutical, and lipid bioaccessibility. *Food & Function*, *9*(1), 22–41. https://doi.org/10.1039/C7FO01515A

McClements, D. J., & Jafari, S. M. (2018). Improving emulsion formation, stability and performance using mixed emulsifiers: A review. *Advances in Colloid and Interface Science*, *251*, 55–79. https://doi.org/10.1016/j.cis.2017.12.001

Mikkonen, K. S., Xu, C., Berton-Carabin, C., & Schroën, K. (2016). Spruce galactoglucomannans in rapeseed oil-in-water emulsions: Efficient stabilization performance and structural partitioning. *Food Hydrocolloids*, *52*, 615–624. https://doi.org/10.1016/j.foodhyd.2015.08.009

Mondal, B., Kote, M., Lunagariya, C., & Patel, M. (2020). Development of a simple high performance liquid chromatography (HPLC)/evaporative light scattering detector (ELSD) method to determine Polysorbate 80 in a pharmaceutical formulation. *Saudi Pharmaceutical Journal*, *28*(3), 325–328. https://doi.org/10.1016/j.jsps.2020.01.012

Muth, M., Rothkötter, S., Paprosch, S., Schmid, R. P., & Schnitzlein, K. (2017). Competition of Thermomyces lanuginosus lipase with its hydrolysis products at the oil–water interface. *Colloids and Surfaces B: Biointerfaces*, *149*, 280–287. https://doi.org/10.1016/j.colsurfb.2016.10.019

Neckebroeck, B., Verkempinck, S. H. E., Vaes, G., Wouters, K., Magnée, J., Hendrickx, M. E., & Van Loey, A. M. (2020). Advanced insight into the emulsifying and emulsion stabilizing capacity of carrot pectin subdomains. *Food Hydrocolloids*, *102*. https://doi.org/10.1016/j.foodhyd.2019.105594

Ngouémazong, E. D., Christiaens, S., Shpigelman, A., Van Loey, A., & Hendrickx, M. (2015). The Emulsifying and Emulsion-Stabilizing Properties of Pectin: A Review. *Comprehensive Reviews in Food Science and Food Safety*, *14*(6), 705–718. https://doi.org/10.1111/1541-4337.12160

763 Nilsson, L., & Bergenståhl, B. (2007). Emulsification and adsorption properties of hydrophobically
764 modified potato and barley starch. *Journal of Agricultural and Food Chemistry*, *55*(4), 1469–1474.
765 https://doi.org/10.1021/jf062087z

766 Pafumi, Y., Lairon, D., de la Porte, P. L., Juhel, C., Storch, J., Hamosh, M., & Armand, M. (2002).
767 Mechanisms of inhibition of triacylglycerol hydrolysis by human gastric lipase. *The Journal of*
768 *Biological Chemistry*, *277*(31), 28070–28079. https://doi.org/10.1074/jbc.M202839200

769 Rabe, M., Kerth, A., Blume, A., & Garidel, P. (2020). Albumin displacement at the air–water interface by
770 Tween (Polysorbate) surfactants. *European Biophysics Journal 2020 49:7*, *49*(7), 533–547.
771 https://doi.org/10.1007/S00249-020-01459-4

772 Reis, P., Holmberg, K., Watzke, H., Leser, M. E., & Miller, R. (2009). Lipases at interfaces: A review. In
773 *Advances in Colloid and Interface Science* (Vols. 147–148, Issue C, pp. 237–250). Elsevier.
774 https://doi.org/10.1016/j.cis.2008.06.001

775 Rodriguez, J. A., Mendoza, L. D., Pezzotti, F., Vanthuyne, N., Leclaire, J., Verger, R., Buono, G.,
776 Carriere, F., & Fotiadu, F. (2008). Novel chromatographic resolution of chiral diacylglycerols and
777 analysis of the stereoselective hydrolysis of triacylglycerols by lipases. *Analytical Biochemistry*,
778 *375*(2), 196–208. https://doi.org/10.1016/J.AB.2007.11.036

779 Rogalska, E., Ransac, S., & Vergers, R. (1990). Stereoselectivity of Lipases II. Stereoselective hydrolysis
780 of triglycerides by gastric and pancreatic lipases. *Journal of Biological Chemistry*, *265*(33), 20271–
781 20276. http://www.jbc.org/

782 Salvia-Trujillo, L., Verkempinck, S. H. E., Sun, L., Van Loey, A. M., Grauwet, T., & Hendrickx, M. E.
783 (2017). Lipid digestion, micelle formation and carotenoid bioaccessibility kinetics: Influence of
784 emulsion droplet size. *Food Chemistry*, *229*, 653–662.
785 https://doi.org/10.1016/j.foodchem.2017.02.146

786 Serdarevich, B. (1967). Glyceride isomerizations in lipid chemistry. *Journal of the American Oil*
787 *Chemists' Society*, *44*(7), 381–393. https://doi.org/10.1007/BF02666775

788 Verkempinck, S. H. E., Kyomugasho, C., Salvia-Trujillo, L., Denis, S., Bourgeois, M., Van Loey, A. M.,
789 Hendrickx, M. E., & Grauwet, T. (2018). Emulsion stabilizing properties of citrus pectin and its
790 interactions with conventional emulsifiers in oil-in-water emulsions. *Food Hydrocolloids*, *85*(3),
791 144–157. https://doi.org/10.1016/j.foodhyd.2018.07.014

792 Verkempinck, S. H. E., Salvia-Trujillo, L., Moens, L. G., Carrillo, C., Van Loey, A. M., Hendrickx, M.
793 E., & Grauwet, T. (2018). Kinetic approach to study the relation between in vitro lipid digestion and
794 carotenoid bioaccessibility in emulsions with different oil unsaturation degree. *Journal of*
795 *Functional Foods*, *41*, 135–147. https://doi.org/10.1016/J.JFF.2017.12.030

796 Verkempinck, S. H. E., Salvia-Trujillo, L., Moens, L. G., Charleer, L., Van Loey, A. M., Hendrickx, M.
797 E., & Grauwet, T. (2018). Emulsion stability during gastrointestinal conditions effects lipid
798 digestion kinetics. *Food Chemistry*, *246*, 179–191.
799 https://doi.org/10.1016/J.FOODCHEM.2017.11.001

800 Wulff-Pérez, M., Gálvez-Ruíz, M. J., de Vicente, J., & Martín-Rodríguez, A. (2010). Delaying lipid
801 digestion through steric surfactant Pluronic F68: A novel in vitro approach. *Food Research*
802 *International*, *43*(6), 1629–1633. https://doi.org/10.1016/j.foodres.2010.05.006

803 Yao, X., Nie, K., Chen, Y., Jiang, F., Kuang, Y., Yan, H., Fang, Y., Yang, H., Nishinari, K., & Phillips,
804 G. O. (2018). The influence of non-ionic surfactant on lipid digestion of gum Arabic stabilized oil-
805 in-water emulsion. *Food Hydrocolloids*, *74*, 78–86. https://doi.org/10.1016/j.foodhyd.2017.07.043

806 Zwietering, M. H., Jongenburger, I., Rombouts, F. M., & Van't Riet, K. (1990). Modeling of the bacterial
807 growth curve. *Applied and Environmental Microbiology*, *56*(6), 1875–1881.
808 https://doi.org/10.1128/aem.56.6.1875-1881.1990

809

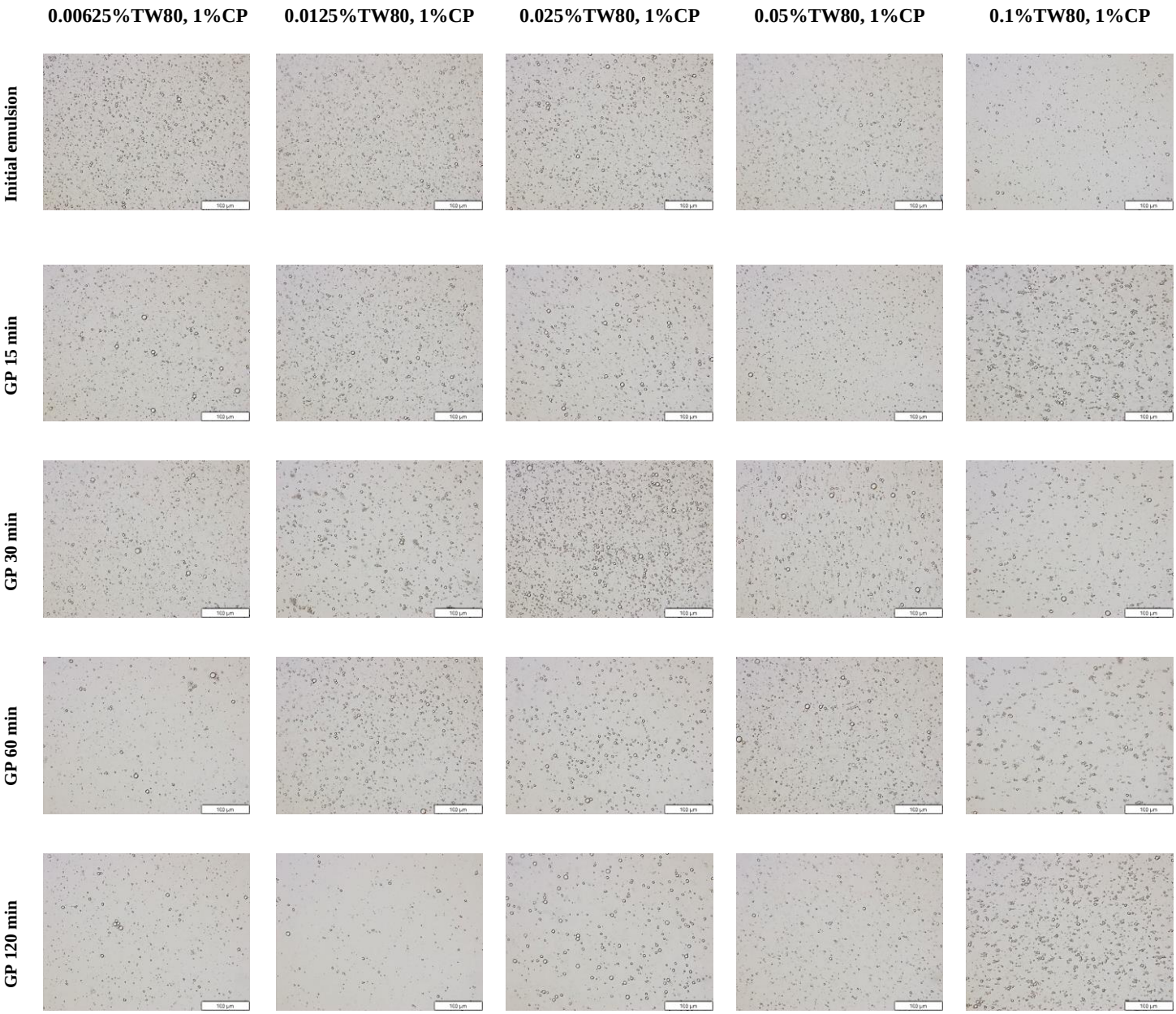

810

811 **Fig. 1.** Microstructural changes of emulsions with mixed interfaces composed of 1% of citrus pectin (CP) and
812 different tween 80 (TW80) concentrations during *in vitro* gastric digestion (GP). Scale bars in the micrographs
813 represent 100 μm.

814

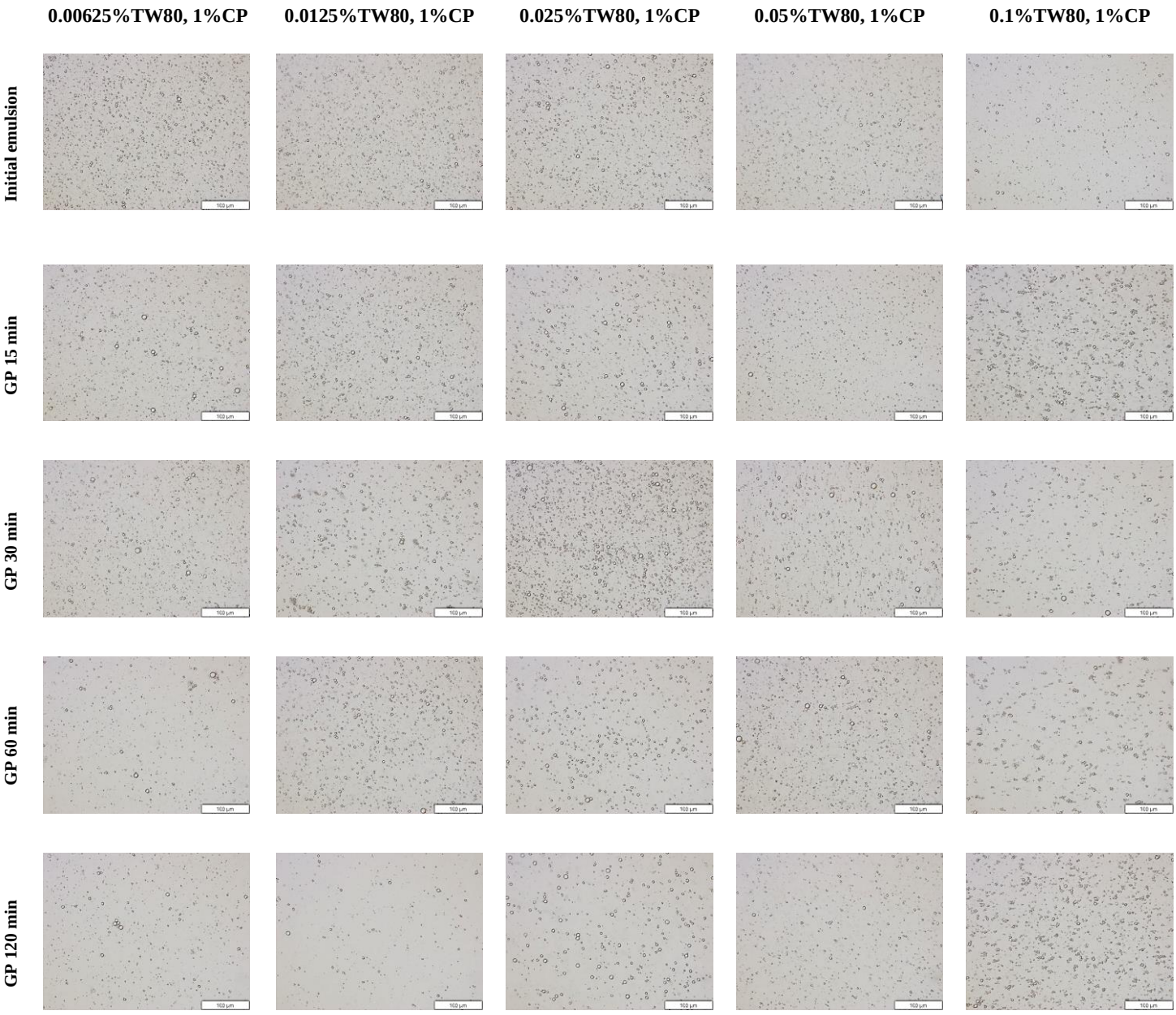

Fig. 1. Microstructural changes of emulsions with mixed interfaces composed of 1% of citrus pectin (CP) and different tween 80 (TW80) concentrations during *in vitro* gastric digestion (GP). Scale bars in the micrographs represent 100 μm.

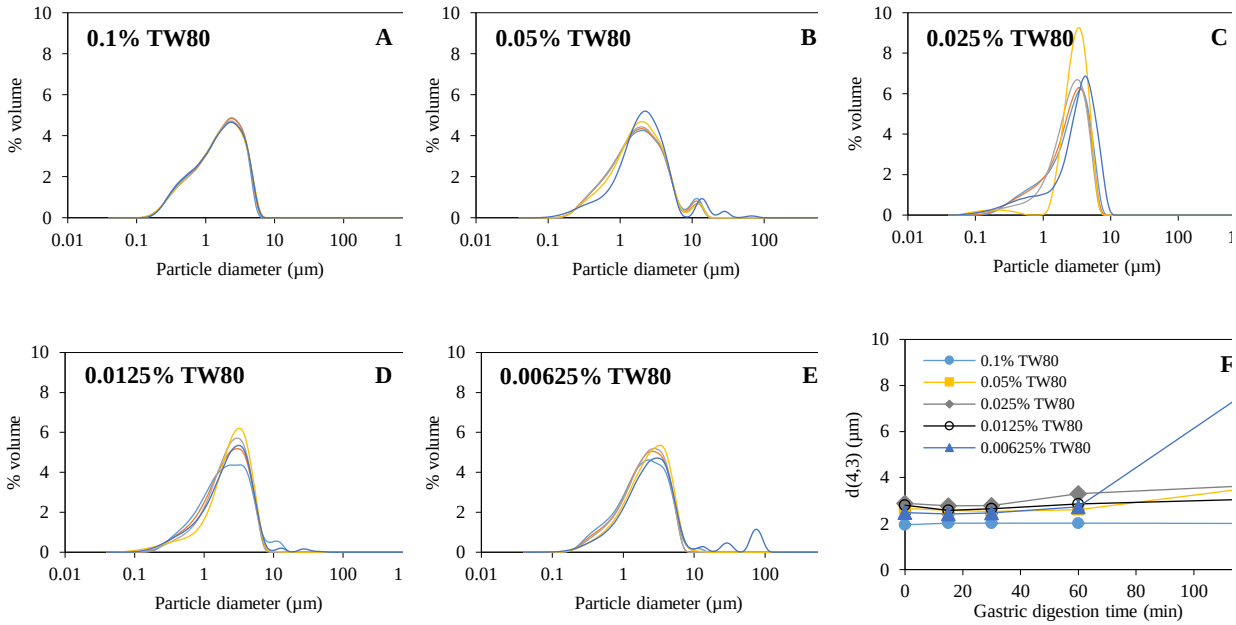
0.1% TW80
A
0.05% TW80
B
0.025% TW80
C
0.0125% TW80
D
0.00625% TW80
E
F
% volume
Particle diameter (µm)
d(4,3) (µm)
Gastric digestion time (min)
0.1% TW80
0.05% TW80
0.025% TW80
0.0125% TW80
0.00625% TW80

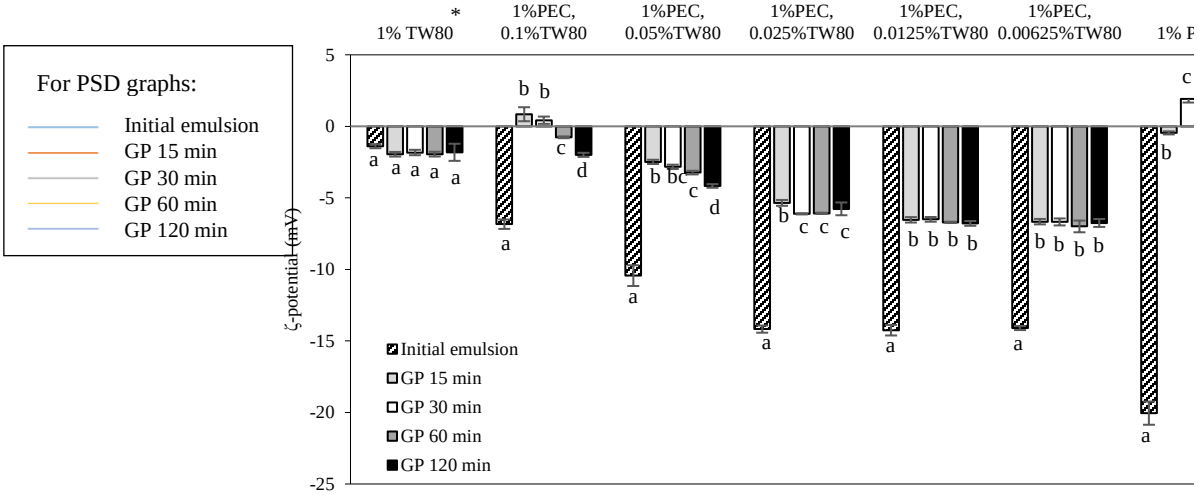
For PSD graphs:
Initial emulsion
GP 15 min
GP 30 min
GP 60 min
GP 120 min
1% TW80
*
1%PEC, 0.1%TW80
1%PEC, 0.05%TW80
1%PEC, 0.025%TW80
1%PEC, 0.0125%TW80
1%PEC, 0.00625%TW80
ζ-potential (mV)

821

822

823

Fig. 2. Time dependency of the (A-E) particle size distribution (PSD), and (F) average volume-based particle size d(4,3) of O/W emulsions stabilized by mixed interfaces composed of 1% of citrus pectin (CP) and different concentrations of tween 80 (TW80) during *in vitro* gastric digestion (GP). (G) Evolution of the ζ-potential of o/w emulsions stabilized by CP and/or TW80 during *in vitro* gastric digestion (GP). For graph G, different lower case letters indicate significant differences ($P < 0.05$) between different digestion times from the same emulsion. *Particle charge values shown in graph G for emulsions individually stabilized by TW80 and CP were taken from our previous study with the permission of Elsevier (Infantes-Garcia et al., 2021).

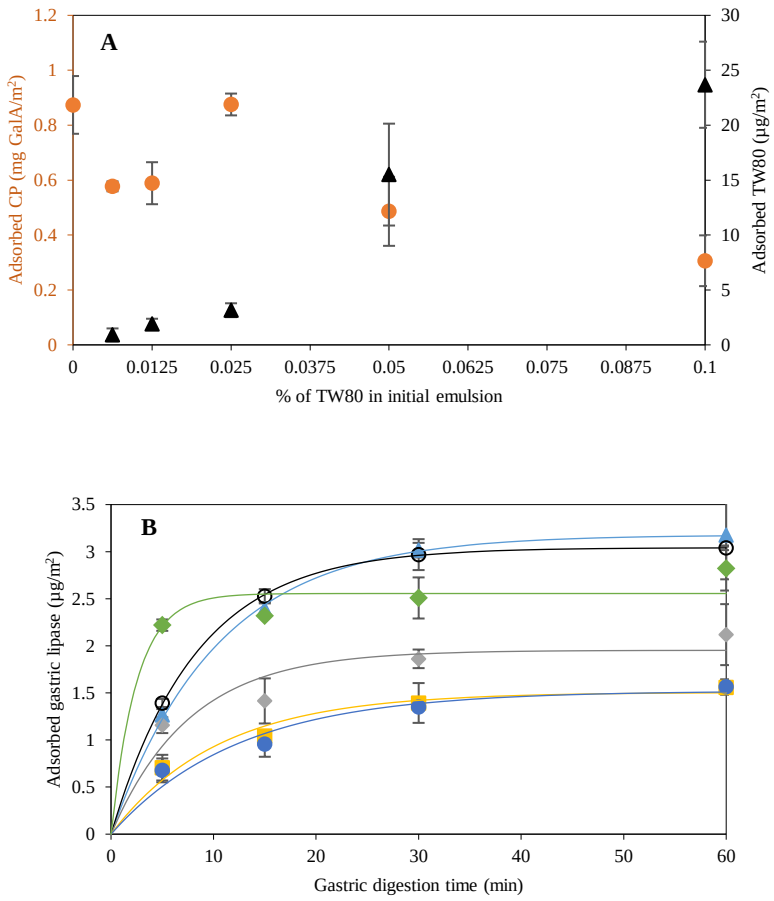

832

833 **Fig. 3.** (A) Adsorbed fractions of citrus pectin (CP, ●) and tween 80 (TW80, ▲) to the oil-water interface as a function
834 of TW80 concentration in initial O/W emulsions stabilized by only CP and mixed interfaces composed of 1% CP and
835 different concentrations of TW80. (B) Evolution of the adsorbed rabbit gastric lipase to the oil-water interface of O/W
836 emulsions stabilized by only CP and mixed interfaces composed of 1% CP and different concentrations of TW80
837 subjected to *in vitro* gastric digestion time. Solid-lines in (B) indicate the fractional conversion model curves
838 representing the kinetics of gastric lipase adsorption. Symbols in (B) indicate concentrations in emulsions prepared
839 with (◆) only 1% CP and mixed interfaces composed of 1% CP and (▲) 0.00625%, (○) 0.0125%, (◆) 0.025%,
840 (■) 0.05%, and (●) 0.1% TW80.

841

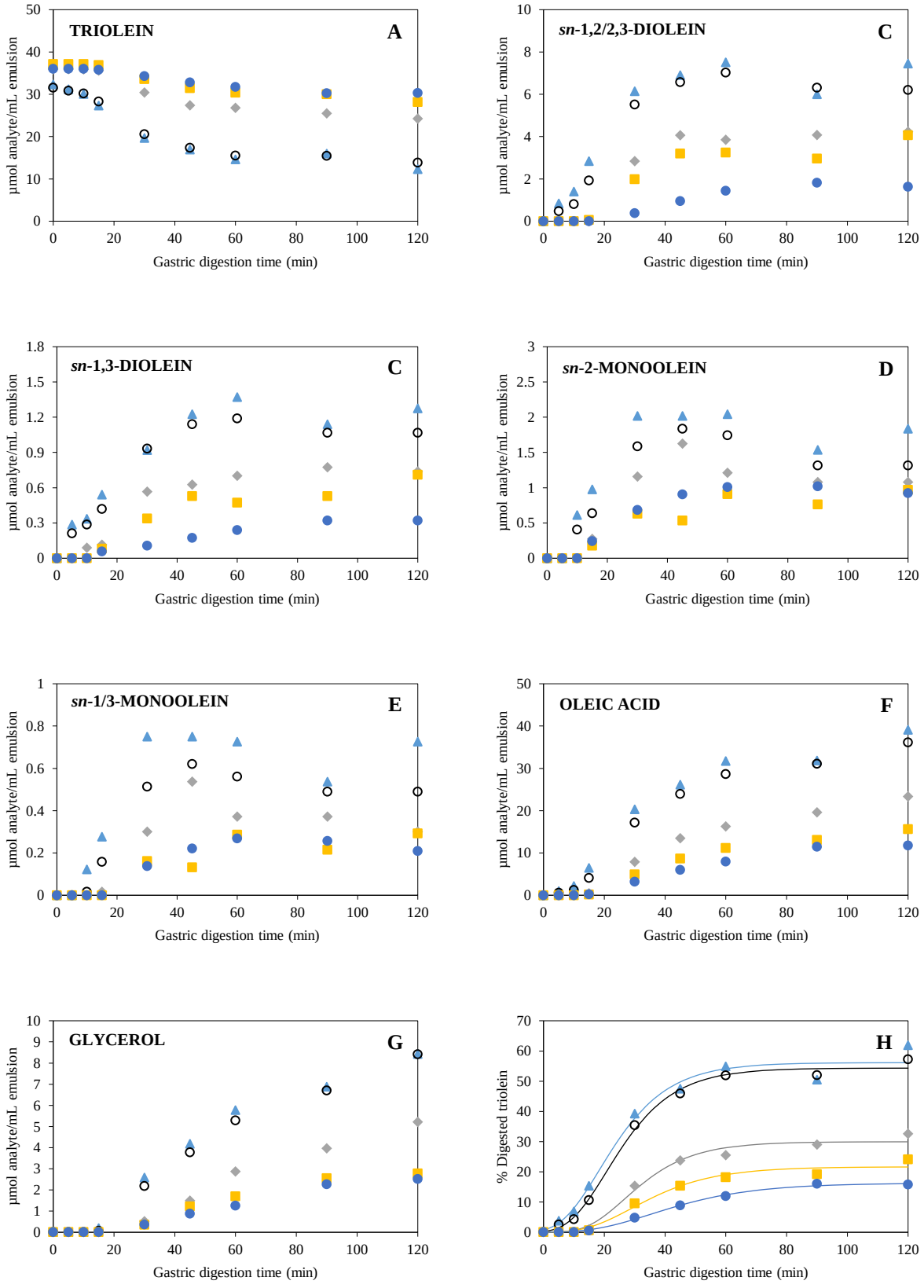
TRIOLEIN
A
µmol analyte/mL emulsion
Gastric digestion time (min)
sn-1,2/2,3-DIOLEIN
C
µmol analyte/mL emulsion
Gastric digestion time (min)
sn-1,3-DIOLEIN
C
µmol analyte/mL emulsion
Gastric digestion time (min)
sn-2-MONOOLEIN
D
µmol analyte/mL emulsion
Gastric digestion time (min)
sn-1/3-MONOOLEIN
E
µmol analyte/mL emulsion
Gastric digestion time (min)
OLEIC ACID
F
µmol analyte/mL emulsion
Gastric digestion time (min)
GLYCEROL
G
µmol analyte/mL emulsion
Gastric digestion time (min)
H
% Digested triolein
Gastric digestion time (min)

842 **Fig. 4.** Molar concentration evolution of (A) triolein and (B, C, D, E, F, G) diverse lipolysis products during *in vitro*
843 gastric digestion, and (H) percentage of digested triolein of emulsions stabilized by mixed interfaces composed of 1%
844 CP and (▲) 0.00625%, (○) 0.0125%, (◆) 0.025%, (■) 0.05%, or (●) 0.1% TW80. Triolein and glycerol were
845 calculated based on the quantified lipid digestion products. Symbols in all graphs represent the experimental analyte
846 concentrations, while solid lines in graph H represent model curves fitted with the modified Gompertz equation.

847

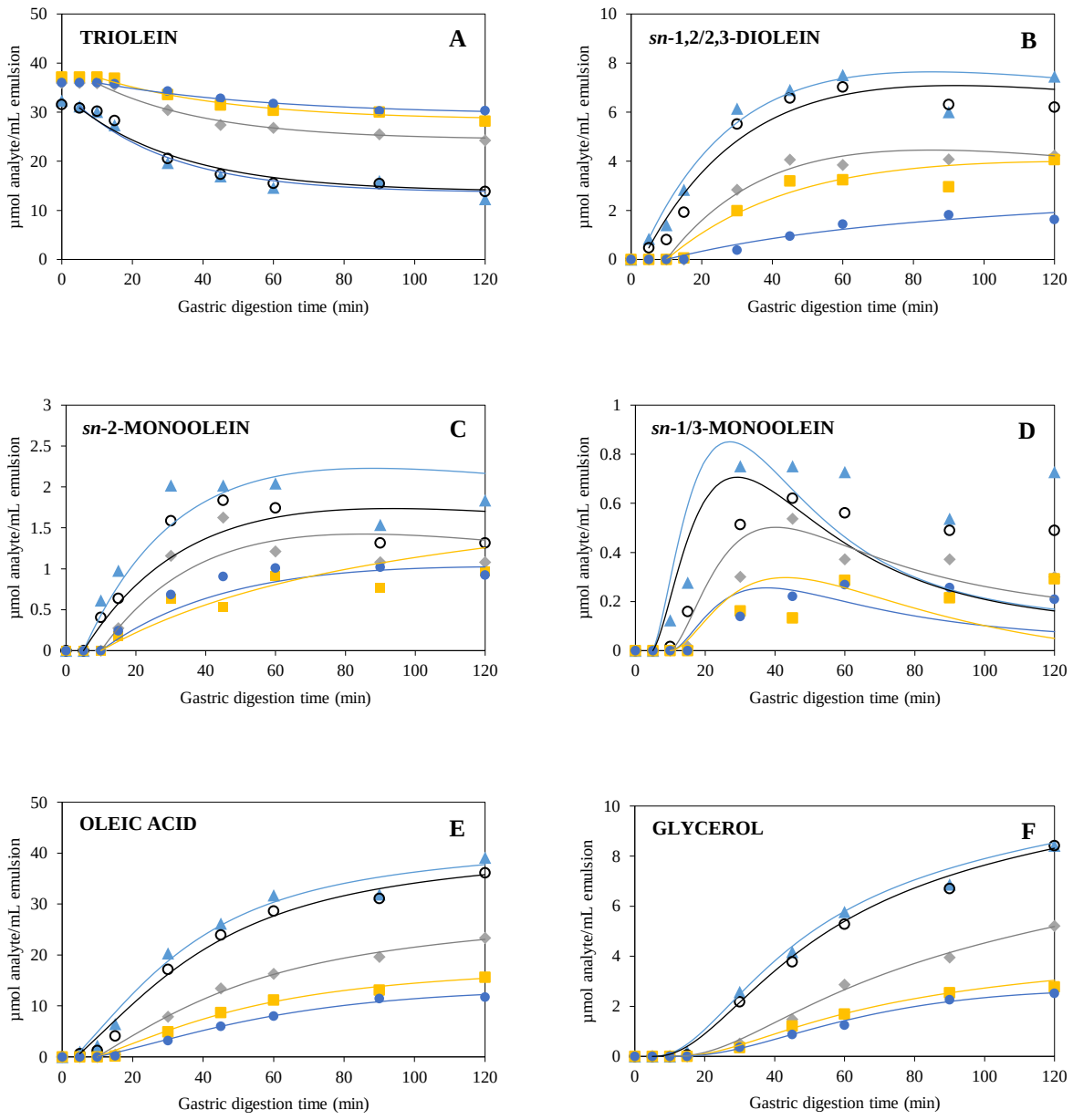

Figure 5. (A, B, C, D, E, F) Representation of the multi-response modeling of emulsions stabilized with mixed interfaces composed of 1% citrus pectin and (▲) 0.00625% tween 80, (○) 0.0125% tween 80, (◆) 0.025% tween 80, (■) 0.05% tween 80, or (●) 0.1% tween 80 subjected to *in vitro* gastric digestion. Triolein and glycerol were calculated based on the quantified lipid digestion products. Symbols in all graphs represent the experimental analyte concentrations for the emulsions. Solid lines in graphs represent the multi-response modeling curves.

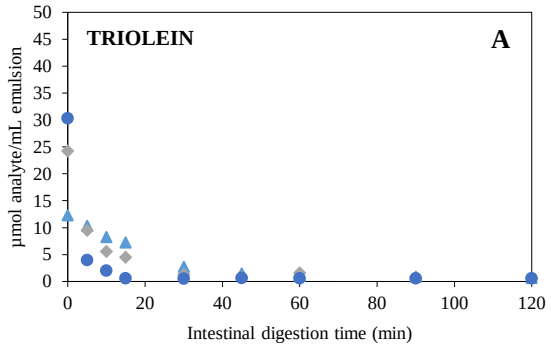
TRIOLEIN
A
µmol analyte/mL emulsion
Intestinal digestion time (min)

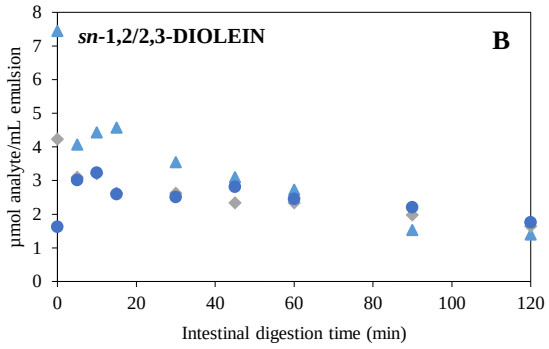
sn-1,2/2,3-DIOLEIN
B
µmol analyte/mL emulsion
Intestinal digestion time (min)

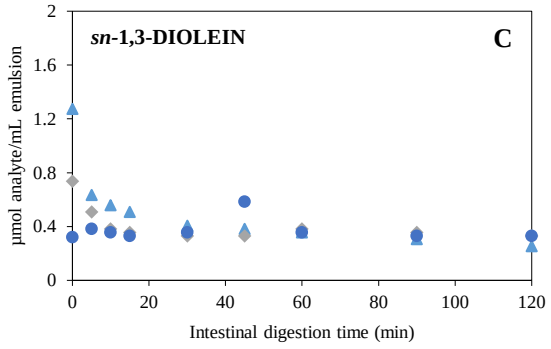
sn-1,3-DIOLEIN
C
µmol analyte/mL emulsion
Intestinal digestion time (min)

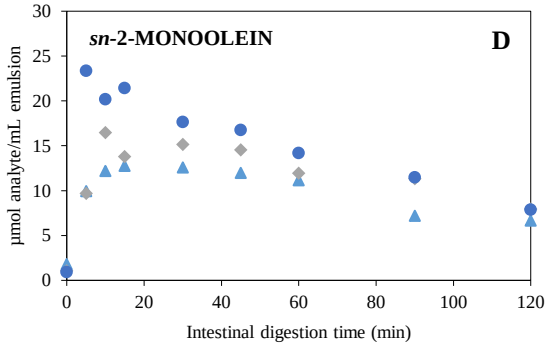
sn-2-MONOOLEIN
D
µmol analyte/mL emulsion
Intestinal digestion time (min)

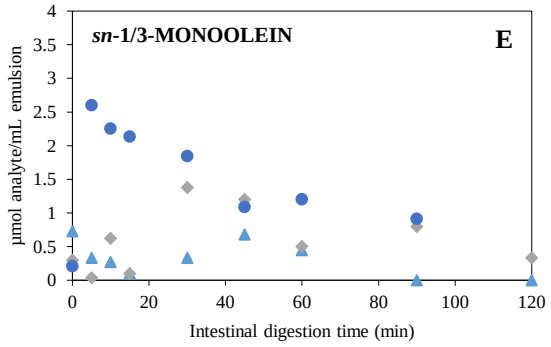
sn-1/3-MONOOLEIN
E
µmol analyte/mL emulsion
Intestinal digestion time (min)

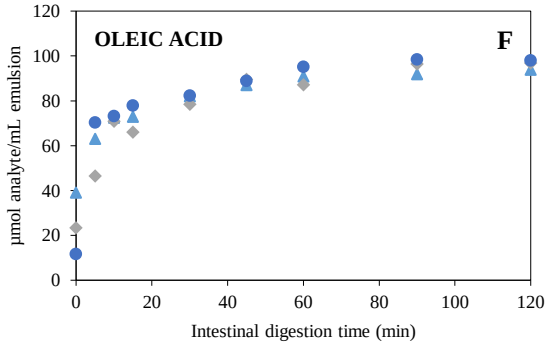
OLEIC ACID
F
µmol analyte/mL emulsion
Intestinal digestion time (min)

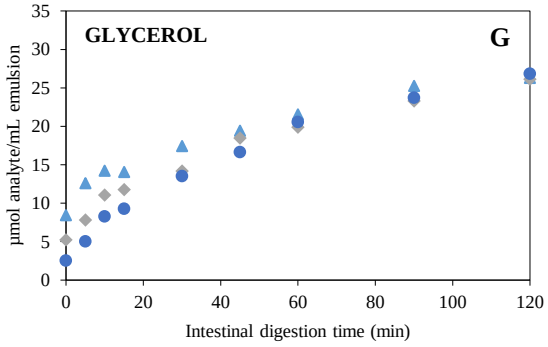
GLYCEROL
G
µmol analyte/mL emulsion
Intestinal digestion time (min)

Fig. 6. Molar concentration evolution of (A) triolein and (B, C, D, E, F, G) diverse lipolysis products during *in vitro* small intestinal digestion of emulsions stabilized by mixed interfaces composed of 1% CP and (▲) 0.00625%, (◆) 0.025%, or (●) 0.1% TW80. Glycerol was calculated based on the quantified lipid digestion products. Symbols in all graphs represent the experimental analytes concentration for the emulsions.

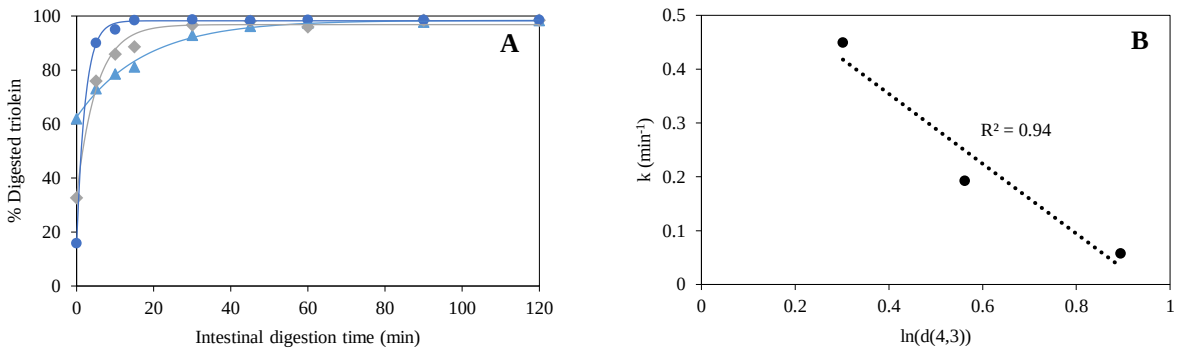

Fig. 7. (A) Percentage of digested triolein of emulsions stabilized by mixed interfaces composed of 1% CP and (▲) 0.00625%, (◆) 0.025%, and (●) 0.1% TW80. (B) Correlation between the average particle size d(4,3) value at the beginning of the intestinal phase and the reaction rate constant *k* (min^{-1}) of digested triolein for emulsions formulated with different mixed emulsifiers. Symbols in graph A represent the experimental analytes concentration for the emulsions while solid lines represent model curves fitted with the fractional conversion equation. In graph B, from left to right, data points correspond to the emulsions prepared with 0.1%, 0.025%, and 0.00625% TW80, respectively.

Table 1. Single-response model parameter estimates of the percentage of digested triolein during *in vitro* gastric digestion of emulsions stabilized by 1% CP and different concentrations of tween 80 (TW80). Different lower case letters indicate significant differences among each parameter estimate according to their confidence intervals (95%). The parameter C_0 is the estimated initial concentration, k is the estimated lipolysis rate constant, and C_f is the estimated final extent of TAG hydrolysis.

	% Digested triolein		
	t_{lag} (min)	k (min $^{-1}$)	H_f (%)
1%CP 0.1%TW80	16.5 ± 1.7^{a}	0.32 ± 0.02^{a}	16.3 ± 0.4^{a}
1%CP 0.05%TW80	14.1 ± 3.8^{a}	0.53 ± 0.10^{b}	21.7 ± 1.2^{b}
1%CP 0.025%TW80	14.3 ± 2.8^{a}	0.89 ± 0.14^{c}	30.0 ± 1.2^{c}
1%CP 0.0125%TW80	8.4 ± 1.2^{b}	1.62 ± 0.13^{d}	54.3 ± 1.1^{d}
1%CP 0.00625%TW80	5.8 ± 2.2^{b}	1.64 ± 0.24^{d}	56.1 ± 2.2^{d}

Table 2. Kinetic parameters estimated through multi-response modeling of the data sets generated after *in vitro* digesting emulsions stabilized by mixed interfaces under gastric conditions. The reaction rate constants for a certain (bio)chemical conversion is represented by k_{number} (min^{-1}), and the final extent of triolein concentration is TAG_f (μM/mL of emulsion). Data sets presented in the table correspond emulsions containing 1% of citrus pectin and different concentrations of tween 80 (TW80). Different lower case letters indicate significant differences among each parameter estimate according to their confidence intervals (95%).

	0.0065% TW80	0.0125% TW80	0.025% TW80	0.05% TW80	0.1% TW80
k_1	0.017 ± 0.002^{a}	0.015 ± 0.002^{a}	0.016 ± 0.002^{a}	0.014 ± 0.002^{a}	0.005 ± 0.001^{b}
k_2	0.013 ± 0.002^{a}	0.013 ± 0.002^{a}	0.010 ± 0.002^{ab}	0.008 ± 0.002^{b}	0.011 ± 0.002^{ab}
k_3	0.005 ± 0.001^{a}	0.004 ± 0.001^{a}	0.005 ± 0.001^{a}	0.004 ± 0.001^{a}	0.004 ± 0.001^{a}
k_4	0.002 ± 0.001^{a}	0.002 ± 0.001^{a}	0.004 ± 0.001^{a}	0.002 ± 0.001^{a}	0.002 ± 0.001^{a}
k_5	0.118 ± 0.052^{a}	0.098 ± 0.038^{a}	0.092 ± 0.039^{a}	0.094 ± 0.053^{a}	0.072 ± 0.025^{a}
k_6	0.002 ± 0.001^{a}	0.002 ± 0.001^{a}	0.001 ± 0.001^{a}	0.002 ± 0.001^{a}	0.002 ± 0.001^{a}
k_7	0.168 ± 0.038^{a}	0.185 ± 0.037^{a}	0.139 ± 0.015^{a}	0.177 ± 0.051^{a}	0.131 ± 0.028^{a}
TAG_f	13.6 ± 0.6^{a}	13.8 ± 0.6^{a}	24.4 ± 0.4^{b}	28.4 ± 0.4^{c}	29.4 ± 0.4^{d}

Table 3. Single-response model parameter estimates of the percentage of digested triolein during *in vitro* small intestinal digestion of emulsions stabilized by 1% CP and different concentrations of tween 80 (TW80). Different lower case letters indicate significant differences among each parameter estimate according to their confidence intervals (95%). The parameter C_0 is the estimated initial concentration, k is the estimated lipolysis rate constant, and C_f is the estimated final extent of TAG hydrolysis.

	% Digested triolein		
	C_0 (%)	k (min^{-1})	C_f (%)
0.00625% TW80	62.5 ± 1.1[a]	0.06 ± 0.01[a]	98.4 ± 0.7[a]
0.025% TW80	33.4 ± 2.7[b]	0.19 ± 0.02[b]	96.8 ± 1.2[a]
0.1% TW80	15.8 ± 1.0[c]	0.45 ± 0.03[c]	98.2 ± 0.4[a]

894

895